Eur. Phys. J. C (2020) 80:155
https://doi.org/10.1140/epjc/s10052-020-7696-1

THE EUROPEAN PHYSICAL JOURNAL C

Regular Article - Experimental Physics

A self-calibrating, double-ratio method to test tau lepton universality in W boson decays at the LHC

S. Dysch, T. R. Wyatt[a]

Particle Physics Group, Department of Physics and Astronomy, University of Manchester, Manchester, UK

Received: 25 October 2019 / Accepted: 29 January 2020 / Published online: 20 February 2020

Abstract Measurements in W^+W^- events at LEP2 and in B hadron semileptonic decays at B factories and LHCb provide intriguing hints of a violation of lepton universality in the charged current coupling of tau leptons relative to those for electrons and muons. We propose a novel, self-calibrating method to test tau lepton universality in W boson decays at the LHC. We compare directly the ratio of the numbers of selected $\ell\tau_{\text{had}}$ and $e\mu$ final states in di-leptonic top quark pair events with that in $Z/\gamma^* \to \tau\tau$ events. Here $\ell = e$ or μ and τ_{had} is a candidate semi-hadronic tau decay. This "double-ratio" cancels to first order sensitivity to systematic uncertainties on the reconstruction of e, μ, and τ leptons, thus improving very significantly the precision to which tau lepton universality can be tested in W boson decay branching ratios at the LHC. Using particle-level Monte Carlo events, and a parameterised simulation of detector performance, we demonstrate the effectiveness of the method and estimate the most significant residual sources of uncertainty arising from experimental and phenomenological systematics. Our studies indicate that a single LHC experiment precision on the tau lepton universality test of around 1.4% is achievable with a data set of $\int L\, \mathrm{d}t = 140\ \mathrm{fb}^{-1}$ at $\sqrt{s} = 13$ TeV. This would improve significantly upon the precision of 2.5% on the four-experiment combined LEP2 measurements. If the central value of the proposed new measurement were equal to the central value of the LEP2 measurement this would yield an observation of BSM physics at a significance level of around 5σ.

1 Introduction

An important feature of the *Standard Model* (SM) of particle physics is *Lepton Universality* (LU): the idea that the *Electroweak* (EW) couplings of the leptons are identical in each fermion generation. For the *Neutral Current* (NC) interactions, mediated in the SM by the γ and Z bosons, the validity of LU for the three flavours of charged leptons (e, μ, τ) has been demonstrated at the scale of the Z boson mass m_Z at LEP1 and SLC to high precision [1]. For example, the ratios of the leptonic partial widths (Γ) or branching fractions ($\mathcal{B}$) of the Z boson are:

$$\begin{aligned} \frac{\Gamma_{\mu\mu}}{\Gamma_{ee}} &\equiv \frac{\mathcal{B}(Z/\gamma^* \to \mu\mu)}{\mathcal{B}(Z/\gamma^* \to ee)} = 1.0009 \pm 0.0028, \\ \frac{\Gamma_{\tau\tau}}{\Gamma_{ee}} &\equiv \frac{\mathcal{B}(Z/\gamma^* \to \tau\tau)}{\mathcal{B}(Z/\gamma^* \to ee)} = 1.0019 \pm 0.0032, \end{aligned} \tag{1}$$

which are consistent with LU to a precision of around three per mille [1]. Measurements of the leptonic asymmetry parameters $\mathcal{A}_\ell$, from forward-backward asymmetries, the left-right asymmetry, and the tau polarisation and its asymmetry:

$$\begin{aligned} \mathcal{A}_e &= 0.1514 \pm 0.0019, \\ \mathcal{A}_\mu &= 0.1456 \pm 0.0091, \\ \mathcal{A}_\tau &= 0.1449 \pm 0.0040, \end{aligned} \tag{2}$$

are also consistent with LU, albeit at the precision of a few percent [1].

In contrast, for the *Charged Current* (CC) interactions, mediated in the SM by the $W^\pm$ bosons, the experimental measurements of leptonic branching ratios are less precise. A direct test of LU at the scale of the W boson mass m_W at LEP2 can be made from the ratios of the leptonic branching fractions of the W boson. The ratio [2]:

$$\frac{\mathcal{B}(W \to \mu\nu)}{\mathcal{B}(W \to e\nu)} = 0.993 \pm 0.019 \tag{3}$$

is consistent with e-μ universality to a precision of around two percent. However a hint at the possible violation of LU in the CC couplings of the τ is present in the ratio [2]:

[a] e-mail: twyatt@fnal.gov (corresponding author)

$$R(W) \equiv \frac{\mathcal{B}(W \to \tau\nu)}{\mathcal{B}(W \to \ell\nu)} = 1.066 \pm 0.025, \quad (4)$$

where $\mathcal{B}(W \to \ell\nu)$ is the average of the branching fractions for $W \to e\nu$ and $W \to \mu\nu$. This result deviates from the assumption of τ-ℓ universality[1] by 2.6σ (standard deviations).

At lower mass scales e-μ universality is tested very precisely, for example in leptonic τ decays the ratio of the muonic and electronic partial widths is measured to be [3]:

$$\frac{\Gamma(\tau^- \to \mu^-\bar{\nu}_\mu\nu_\tau)}{\Gamma(\tau^- \to e^-\bar{\nu}_e\nu_\tau)} = 0.9762 \pm 0.0028, \quad (5)$$

which is consistent with the SM prediction including mass effects of 0.9726 [3]. e-μ universality is also tested in the decays of charged kaons [3]:

$$\frac{\Gamma(K^- \to e^-\bar{\nu}_e)}{\Gamma(K^- \to \mu^-\bar{\nu}_\mu)} = (2.488 \pm 0.009) \times 10^{-5}, \quad (6)$$

which is consistent with the SM prediction [4] of 2.477×10^{-5}.

In the decay of B hadrons, τ-ℓ universality can be tested by measurements of the branching fractions for the exclusive decays of $\overline{B}^0 \to \tau^-\overline{\nu}_\tau D^+$ and $\overline{B}^0 \to \tau^-\overline{\nu}_\tau D^{*+}$ expressed as ratios to the branching fractions for the exclusive decays $\overline{B}^0 \to \ell^-\overline{\nu}_\ell D^+$ and $\overline{B}^0 \to \ell^-\overline{\nu}_\ell D^{*+}$, respectively. Systematic uncertainties due to hadronic effects largely cancel in these ratios. A combination [5] of the results from the BaBar [6,7], Belle [8–12], and LHCb [13–16] experiments yields the results:

$$\begin{aligned} R(D) &\equiv \frac{\mathcal{B}(\overline{B}^0 \to \tau^-\overline{\nu}_\tau D^+)}{\mathcal{B}(\overline{B}^0 \to \ell^-\overline{\nu}_\ell D^+)} = 0.340 \pm 0.027 \pm 0.013, \\ R(D^*) &\equiv \frac{\mathcal{B}(\overline{B}^0 \to \tau^-\overline{\nu}_\tau D^{*+})}{\mathcal{B}(\overline{B}^0 \to \ell^-\overline{\nu}_\ell D^{*+})} = 0.295 \pm 0.011 \pm 0.008. \end{aligned} \quad (7)$$

These measured values exceed the SM predictions (calculated assuming LU) of:

$$\begin{aligned} R(D) &= 0.300 \pm 0.008, \\ R(D^*) &= 0.252 \pm 0.003, \end{aligned} \quad (8)$$

by 1.4σ and 2.5σ respectively (see [5] and the references contained therein). Taking into account correlations between the measurements, the combined discrepancy with regard to the SM predictions corresponds to 3.1σ [5].

[1] In this paper the symbol ℓ is taken to denote an electron (e) or a muon (μ), but not a tau (τ) lepton.

Possible *Beyond the Standard Model* (BSM) explanations have been proposed for the potential violation of LU in $R(D)$ and $R(D^*)$. A *Leptoquark* (LQ) that couples more strongly to the τ than to e or μ could contribute at tree level to the decays $\overline{B}^0 \to \tau^-\overline{\nu}_\tau D^{(*)+}$. For example, in [17] a charge 2/3 scalar LQ with $b\tau$ and $c\nu$ Yukawa couplings is able to accommodate the measured central values of $R(D)$ and $R(D^*)$ without introducing an unacceptable level of flavour changing neutral current processes involving the first two generations of quarks and leptons. Interestingly, a possible link between the LEP2 measurement of $R(W)$ and the $\overline{B}^0 \to \tau^-\overline{\nu}_\tau D^{(*)+}$ excess has received little attention in the literature. We note that $R(W)$ might receive contributions at loop level from a LQ that couples preferentially to the τ. For example, if cs and $s\tau$ Yukawa couplings were added to the charge 2/3 LQ scenario of [17] it could produce an enhancement in $\mathcal{B}(W \to \tau\nu)$. Such loop-level contributions might naturally lead to a smaller fractional deviation from LU in $R(W)$ than in $R(D)$ and $R(D^*)$, but this would depend, obviously, on the sizes of the assumed couplings.

Clearly it is important to improve on the precision of the measurements of $R(W)$ [currently 2.5%], $R(D)$ [currently 11%] and $R(D^*)$ [currently 5%]. The precision of the LEP2 measurement of $R(W)$ was dominated by the limited number of available W^+W^- events. A future high energy, high luminosity e^+e^- collider, at which an improved $R(W)$ measurement could be performed, is likely to be decades away.

Measurements at hadron colliders that are sensitive to $R(W)$ usually rely on the identification of τ lepton decays in which the visible final state is hadronic (τ_{had}). The current best published hadron collider measurements typically have small statistical uncertainties, but are dominated by large systematic uncertainties that render them uncompetitive with the LEP2 measurement of $R(W)$. For example, a measurement of the inclusive single $W \to \tau_{\text{had}}\nu$ cross section in pp collisions at 7 TeV by ATLAS [18] has a relative uncertainty of 15%, which is dominated by systematic uncertainties on the efficiency to trigger on and select events containing τ_{had} candidates.

Also of interest in this context are measurements at hadron colliders of the rate of events containing top quark–antiquark pairs (tt), especially in the di-lepton final state. For the purpose of determining $R(W)$ events containing top quarks may be regarded as a convenient source of on-mass-shell W bosons. In the absence of non-SM decay mechanisms for the top quark the branching fraction $\mathcal{B}(t \to b\tau\nu)$ may be reinterpreted as the branching fraction $\mathcal{B}(W \to \tau\nu)$.

Relative to measurements of the inclusive single $W \to \tau_{\text{had}}\nu$ cross section, measurements using di-leptonic $tt \to bb\ell\tau_{\text{had}}$ events eliminate systematic uncertainties associated with the trigger efficiencies for τ_{had} candidates, because single-ℓ (e or μ) triggers can be used. In addition, non-tt

backgrounds can be almost completely eliminated from the $tt \to bb\ell\tau_{\text{had}}$ final state by employing b-jet tagging and the presence of the ℓ candidate. This means that the background from misidentified hadronic jets to the τ_{had} signature in the $tt \to bb\ell\tau_{\text{had}}$ final state is likely to be significantly smaller than that in the inclusive single $W \to \tau_{\text{had}}\nu$ final state. However, systematic uncertainties associated with the τ_{had} candidate (identification efficiency, background and energy scale) still contribute directly to the measured rate of $tt \to bb\ell\tau_{\text{had}}$ events. For example, in a measurement by ATLAS [19] in dileptonic tt events the systematic uncertainty on the branching fraction $\mathcal{B}(t \to b\tau\nu)$ is around 7.5%. In a measurement by CMS of the cross section for the $tt \to bb\ell\tau_{\text{had}}$ final state [20], the systematic uncertainty is around 9.5%; to which the combined contribution from the identification efficiency (6.0%), background (4.3%), and energy scale (2.5%) for τ_{had} candidates was 7.8%. In the above-mentioned best currently published measurements from ATLAS [19] and CMS [20] based on the $tt \to bb\ell\tau_{\text{had}}$ final state the systematic uncertainties associated with the τ_{had} candidate are around a factor of three greater than total uncertainty of 2.5% on the LEP2 measurement of $R(W)$.

We propose here a novel, self-calibrating, "double-ratio" method that will allow $R(W)$ to be measured using top quark pair ($t\bar{t} \to b\bar{b}W^+W^-$) and $Z/\gamma^* \to \tau\tau$ events at the LHC with a target precision of around 1%, which would improve significantly upon the LEP2 measurements. We define the ratio:

$$R(bbWW) \equiv \frac{N(tt \to bb\ell\tau_{\text{had}})}{N(tt \to bbe\mu)}, \tag{9}$$

where $N(tt \to bb\ell\tau_{\text{had}})$ and $N(tt \to bbe\mu)$ are the numbers of observed candidate events in the $tt \to bb\ell\tau_{\text{had}}$ and $tt \to bbe\mu$ final states, respectively. We define also the ratio:

$$R(Z) \equiv \frac{N(Z \to \tau\tau \to \ell\tau_{\text{had}})}{N(Z \to \tau\tau \to e\mu)}, \tag{10}$$

where $N(Z \to \tau\tau \to \ell\tau_{\text{had}})$ and $N(Z \to \tau\tau \to e\mu)$ are the numbers of observed candidate events in the $Z \to \tau\tau \to \ell\tau_{\text{had}}$ and $Z \to \tau\tau \to e\mu$ final states, respectively. We then define the double ratio:

$$\begin{aligned} R(WZ) &\equiv \frac{R(bbWW)}{R(Z)} \\ &\equiv \frac{N(tt \to bb\ell\tau_{\text{had}}) \times N(Z \to \tau\tau \to e\mu)}{N(tt \to bbe\mu) \times N(Z \to \tau\tau \to \ell\tau_{\text{had}})} \end{aligned} \tag{11}$$

From an experimental perspective we note that the ratios $R(bbWW)$ and $R(Z)$ are designed to have approximately the same sensitivity to systematic uncertainties on the identification of e, μ and τ_{had} candidates, and on the efficiencies of the single-ℓ triggers. Therefore, in the double ratio $R(WZ)$ these systematic uncertainties cancel to first order. This cancellation is not necessarily perfect for the following reasons.

- The distributions in *transverse momentum* (p_T) and *pseudorapidity* (η) [21] of the leptons (e, μ and τ) are significantly different in the $t\bar{t} \to b\bar{b}W^+W^-$ and $Z/\gamma^* \to \tau\tau$ signal samples. Systematic uncertainties on lepton identification and single-ℓ trigger efficiencies are not necessarily fully correlated across all p_T and $|\eta|$ bins.
- The levels of background from misidentified hadronic jets in the τ_{had} candidates in the $tt \to bb\ell\tau_{\text{had}}$ and $Z \to \tau\tau \to \ell\tau_{\text{had}}$ samples are not necessarily identical.
- The level and nature of the non-tt background in the $tt \to bb\ell\tau_{\text{had}}$ and $tt \to bbe\mu$ samples will not necessarily be identical. Similarly, the level and nature of the non-Z boson background in the $Z \to \tau\tau \to \ell\tau_{\text{had}}$ and $Z \to \tau\tau \to e\mu$ samples will not necessarily be identical.

From a phenomenological perspective the double ratio $R(WZ)$ exploits the fact that LU has been precisely verified experimentally in the Z boson branching fractions (see equation 1). Therefore, any non-SM effects should affect $R(WZ)$ primarily through $R(bbWW)$, which is sensitive to $R(W)$.

The rest of this paper is organised as follows. In Sect. 2 we describe a *Monte Carlo* (MC) study of the proposed analysis method employing a simple parameterised simulation of detector performance. In Sect. 3 we present our summary and conclusions.

2 A Monte Carlo study of the proposed double-ratio analysis method

Our study uses particle-level MC events for the various physics processes of relevance. In Sect. 2.1 we describe briefly the simple parameterised simulation of detector performance we use in the study of the proposed double-ratio analysis method. We describe also the variations in detector performance we consider in the study of experimental systematic uncertainties. Further details are given in the Appendix. In Sect. 2.2 we describe the MC generators used and the potential sources of phenomenological systematic uncertainties that we have considered in our study. In Sect. 2.3 we describe the candidate event selection criteria we employ for the four signal candidate event samples used in the double-ratio method. In the selection of $Z/\gamma^* \to \tau\tau$ candidates we propose a novel selection variable, m_3^*, that improves the discrimination power against the dominant backgrounds, such as tt, diboson production, as well as events containing a leptonically decaying vector boson plus a QCD jet that is misidentified as a τ_{had} candidate (W+jet). In Sect. 2.4 we evaluate the size and composition of the four selected candidate event samples. The

expected numbers of events are given for an integrated luminosity at $\sqrt{s} = 13$ TeV of $\int L\, dt = 140\ \text{fb}^{-1}$, which corresponds approximately to that available for physics analysis in ATLAS and CMS at the end of LHC run 2 [22,23]. In Sect. 2.5 we evaluate the sensitivity of the measured double ratio $R(WZ)$ to the physical quantity of interest $R(W)$. In Sect. 2.6 we present the effect of systematic uncertainties on the ratios $R(bbWW)$, $R(Z)$, $R(WZ)$, and $R(W)$. We thus demonstrate that in the double-ratio $R(WZ)$ there is a high degree of cancellation in the experimental systematic uncertainties that have dominated previous related analyses at hadron colliders. We evaluate the residual systematic uncertainties on $R(WZ)$ arising from the effects discussed in Sects. 2.1 and 2.2. In Sect. 2.7 we discuss some limitations of this simplified study and consider some factors that will need to be taken into account in an analysis that uses detailed simulations of a specific LHC detector and is applied to the experimental data.

2.1 Simple parameterised Monte Carlo simulation of detector performance

In this section we describe briefly the simple parameterised simulation of detector performance we use to study the proposed double-ratio analysis method. We describe also the variations in detector performance we consider in the study of systematic uncertainties.

Clearly, our aim here is not to produce a completely accurate simulation of the data from either the ATLAS or CMS detectors. Nevertheless, we base our parameterisations of the detection of leptons and jets on published measurements of LHC detector performance and their associated uncertainties [24,55]. This approach enables us to demonstrate some of the principle benefits of the proposed double-ratio method and allows us to investigate within a simple and controlled framework the principal sources of residual systematic uncertainty to which the method is sensitive.

The efficiencies associated with the reconstruction, identification, and triggering of high p_T, isolated lepton candidates are typically determined by the ATLAS and CMS collaborations using "tag and probe" measurements on $Z \to ee, \mu\mu, \tau\tau$ events in both MC simulations and the real data. Systematic uncertainties are usually quoted on the "scale factors" employed to correct MC simulations to provide an accurate description of the real data.

As noted in Sect. 1, the ratios $R(bbWW)$ and $R(Z)$ are designed to have approximately the same sensitivity to systematic uncertainties on the identification of e, μ and τ_{had} candidates, and on the efficiencies of the single-ℓ triggers. In the double ratio $R(WZ)$, these systematic uncertainties cancel to first order. Therefore, in our study we give particular attention to the p_T and η dependence of efficiencies and to any potential p_T and η dependence in the associated systematic uncertainties. In general we expect algorithms that are designed to have p_T- and η-independent efficiencies to have smaller p_T- and η-dependent systematic uncertainties.

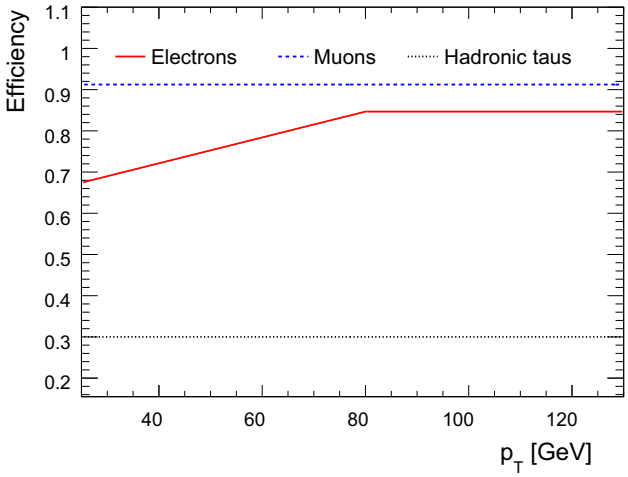

Fig. 1 The overall efficiencies assumed for the reconstruction, identification, and isolation criteria for prompt e, μ, and τ_{had} candidates as a function of p_T

Figure 1 shows as a function of p_T the overall efficiencies we assume for the reconstruction, identification, and isolation criteria for prompt e, μ, and τ_{had} candidates. Table 1 gives a summary of the sources of systematic uncertainty on the reconstruction of leptons and jets considered in this study, stating separately the assumed size of the p_T/η-independent and p_T/η-dependent systematic uncertainties. Figure 2 shows the p_T-dependent systematic uncertainties on the efficiencies we assume for the reconstruction, identification, and isolation criteria for prompt e, μ, and τ_{had} candidates.

Jets with $|\eta| < 2.5$ are flagged as b-tagged with probabilities that depend on their flavour at truth level as follows: truth b 85%, truth c 40%, truth light quark or gluon 1%. These tag probabilities are approximately independent of p_T and $|\eta|$.

A detailed description of our choices of lepton and jet identification algorithms to simulate and experimental systematic uncertainties to consider, and the reasoning behind these choices, are given in the Appendix.

2.2 Monte Carlo generators and phenomenological systematic uncertainties

Events containing W bosons, Z bosons, top quark pairs, and the EW production of single top quarks are generated using POWHEG BOX [56], interfaced to PYTHIA[57] for the simulation of parton showering and fragmentation. We thus ensure a consistent treatment of tau lepton decay in the principle sources of candidate events. EW diboson events are generated using SHERPA [58].

Table 1 Sources of experimental systematic uncertainty, together with the size (in percent, unless stated otherwise) of the p_T/η-independent and p_T/η-dependent systematic uncertainties considered in this study. In all expressions p_T is given in units of GeV. We define the endcap region by $|\eta| > 1.0$. See the Appendix for further detail and justification of these choices

Source of	Size of systematic uncertainty (in %, unless stated otherwise)	
Systematic uncertainty	p_T/η-independent	p_T/η-dependent
Muon ID & isolation efficiency	2.0	$0.5\left(\frac{80-p_T}{50}\right)$, 0 for $p_T > 80$ GeV
Single-muon trigger efficiency	1.0	1.0 in endcap, 0 in barrel
Muon p_T resolution	0.15	0.15 in endcap, 0 in barrel
Muon p_T scale	0.2	0.2 in endcap, 0 in barrel
Electron ID & isolation efficiency	2.0	$2.0\left(\frac{80-p_T}{50}\right)$, 0 for $p_T > 80$ GeV
Single-electron trigger efficiency	1.0	1 GeV change in p_T threshold
Electron p_T resolution	Vary constant term in $\frac{\sigma_{p_T}}{p_T}$ by ± 0.002	Vary resolution in endcap only
Electron p_T scale	0.2	0.2 in endcap, 0 in barrel
τ_{had} efficiency	5	$5\left(\frac{130-p_T}{100}\right)$, 0 for $p_T > 130$ GeV
τ_{had} p_T scale	1	1 in endcap, 0 in barrel
jet energy scale	1	–
b-tag efficiency for b-, c-, light-jets	1.5, 4, 10	–
Misidentification rates for τ_{had}	10	–
MJ background in $Z \to \tau\tau \to \ell\tau_{\text{had}}$ sample	5	–

Significant sources of background in the selected $Z/\gamma^* \to \tau\tau$ samples arise from EW diboson and tt production. Cross sections at $\sqrt{s} = 13$ TeV have been measured for EW diboson [59] and tt [60] production. Our estimates of the fractional composition of the selected $Z/\gamma^* \to \tau\tau$ samples are not sensitive to systematic uncertainties on the integrated luminosity or on the predicted absolute cross sections for Z boson, tt, or EW diboson production. They are, however, sensitive to systematic uncertainties on the ratio of the cross sections for tt and EW diboson production to that for Z bosons. We assume an uncertainty of 3% on both of these cross section ratios [61].

In $Z/\gamma^* \to \tau\tau$ events the momentum distribution of electrons and muons produced in τ decay is softer than that for the visible τ_{had} systems. Changes in the distribution of the transverse momentum of the produced Z bosons ($p_T(Z)$) can, therefore, affect the relative acceptance for $Z \to \tau\tau \to \ell\tau_{\text{had}}$ and $Z \to \tau\tau \to e\mu$ candidate events. Measurements of $p_T(Z)$ have been made at $\sqrt{s} = 8$ TeV by ATLAS [62]. In order to evaluate systematic uncertainties arising from $p_T(Z)$ we increase the weight of events satisfying 50 GeV $< p_T(Z) <$ 150 GeV by 0.5% and the weight of events satisfying $p_T(Z) > 150$ GeV by 1.0% [63].

In $tt \to bb\ell\tau_{\text{had}}$ events, the majority of observed electrons and muons are from direct W boson decays and therefore have a distribution in p_T that is much harder than that for the visible τ_{had} systems. The relative acceptance for $tt \to bb\ell\tau_{\text{had}}$ and $tt \to bbe\mu$ final states may be sensitive to the details of the modelling of tt production. We investigate this sensitivity by using an alternative tt generator-level sample in which the QCD factorisation and renormalisation scales are changed by a factor of two relative to the default values. In addition, we evaluate systematic uncertainties arising from simulating the distribution of the mass of the tt sys-

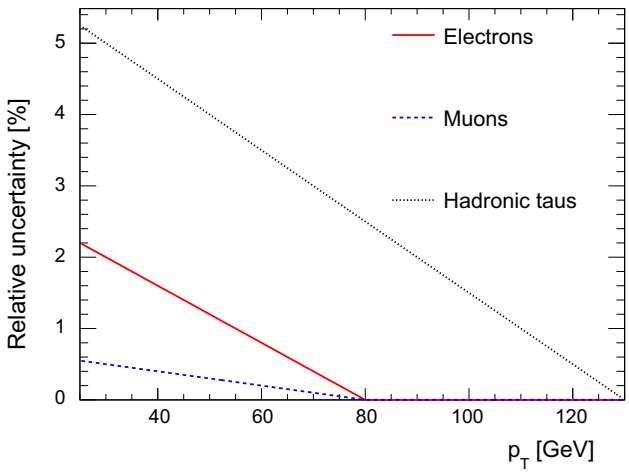

Fig. 2 The p_T-dependent systematic uncertainties on the efficiencies we assume for the reconstruction, identification, and isolation criteria for prompt e, μ, and τ_{had} candidates

Table 2 Sources of phenomenological systematic uncertainty considered in this study (given in percent). In all expressions, p_T and $m(t\bar{t})$ are given in units of GeV. See the text for further details

Source of systematic uncertainty	Size of fractional systematic uncertainty (in %)
Ratio of diboson and Z boson cross sections	3
Ratio of tt and Z boson cross sections	3
$p_T(Z)$ reweighting	0.5 for $50 < p_T(Z) < 150$
	1.0 for $p_T(Z) > 150$
$m(t\bar{t})$ reweighting	$10 + 0.018(m(t\bar{t}) - 1000)$
tt modelling	Tested with alternative sample

tem, $m(t\bar{t})$, by increasing the weights of events by an amount that varies linearly between 1% at $m(t\bar{t})$ = 500 GeV to 10% at $m(t\bar{t})$ = 1000 GeV [65].

Table 2 gives a summary of the sources of phenomenological systematic uncertainty considered in this study.

2.3 Candidate event selection criteria

Candidate electrons and muons are considered in the analysis if after simulation of resolution and momentum scale they satisfy $p_T > 27$ GeV. Candidate τ_{had} and hadronic jets are considered if after simulation of resolution and momentum scale they satisfy $p_T > 25$ GeV. Hadronic jets must satisfy $|\eta| < 4.5$. Candidate electrons, muons, τ_{had}, and b-tagged jets must satisfy $|\eta| < 2.5$.

2.3.1 Candidate event selection criteria on leptons

In order to maximise the cancellation of systematic uncertainties between $t\bar{t} \to b\bar{b}W^+W^-$ and $Z/\gamma^* \to \tau\tau$ event samples the same candidate event selection criteria on leptons are applied in the two event classes.
Candidate $e\tau_{\text{had}}$ events are required to contain:

- Exactly one e candidate.
- Exactly one τ_{had} candidate of opposite sign to the e candidate.
- No μ candidates.
- The e candidate must fire the single-e trigger.

Candidate $\mu\tau_{\text{had}}$ events are required to contain:

- Exactly one μ candidate.
- Exactly one τ_{had} candidate of opposite sign to the μ candidate.
- No e candidates.
- The μ candidate must fire the single-μ trigger.

Candidate $e\mu$ events are required to contain:

- Exactly one e candidate.
- Exactly one μ candidate of opposite sign to the e candidate.
- The e candidate must fire the single-e trigger, and/or the μ candidate must fire the single-μ trigger.

2.3.2 tt candidate event selection criteria

In addition to the relevant criteria on leptons given in Sect. 2.3.1 above, all candidate $t\bar{t} \to b\bar{b}W^+W^-$ events ($tt \to bb\ell\tau_{\text{had}}$ as well as $tt \to bbe\mu$) are required to contain exactly two b-tagged jets. Because the same criterion is applied in the selection of the numerator $tt \to bb\ell\tau_{\text{had}}$ and denominator $tt \to bbe\mu$ events, we expect the ratio $R(bbWW)$ to be largely insensitive to systematic uncertainties associated with jet reconstruction, JES, JER, and b-tagging. Requiring two b-tagged jets reduces the background in the selected $t\bar{t} \to b\bar{b}W^+W^-$ event samples from non-tt sources; it also reduces the background from tt events in which a b-quark jet is misidentified as a prompt e, μ, or τ_{had}.

Candidate $tt \to bb\ell\tau_{\text{had}}$ events are rejected if the invariant mass of the τ_{had} candidate and the highest p_T non-b-tagged jet, $m(j - \tau_{\text{had}})$, satisfies 50 GeV $< m(j - \tau_{\text{had}}) < 90$ GeV. This criterion reduces the background from lepton+jet tt events in which the hadronically decaying W boson produces two reconstructed jets, one of which is misidentified as a τ_{had} candidate. The effectiveness of this criterion is illustrated by Fig. 3, which shows in the $tt \to bb\ell\tau_{\text{had}}$ candidate event sample the distribution of $m(j - \tau_{\text{had}})$, having applied all other $tt \to bb\ell\tau_{\text{had}}$ event selection criteria. The upper plot shows events in which the τ_{had} candidate originates from a genuine τ decay and the lower plot shows events in which the τ_{had} candidate originates from a misidentified hadronic jet. A clear peak at around the mass of the W boson can be seen in the lower plot. In addition to helping reject background from misidentified hadronic jets, the distributions in Fig. 3 offer the possibility to make a data-driven estimate of the background in the τ_{had} candidate sample. This will be useful in reducing the systematic uncertainty on the background yield.

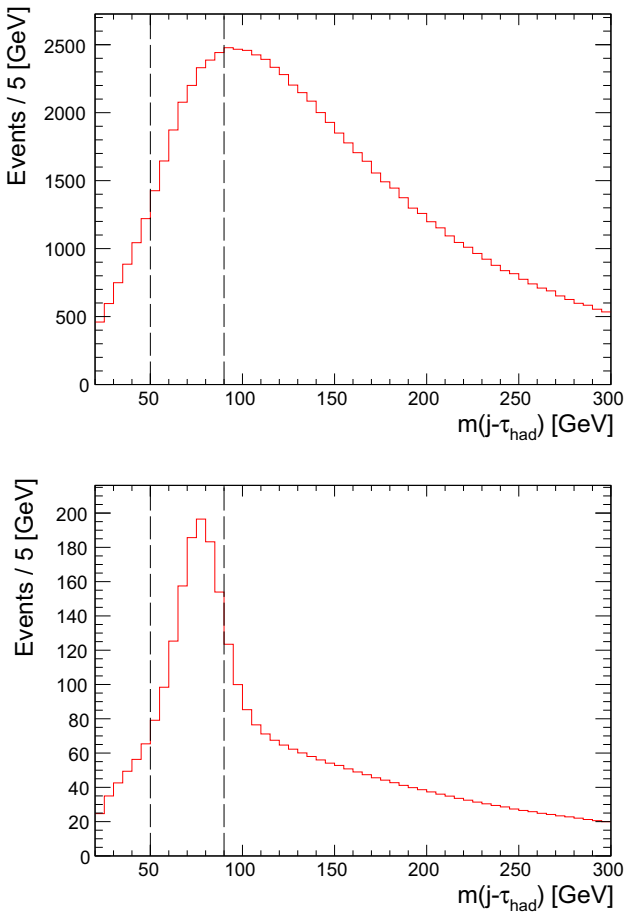

Fig. 3 The distribution of $m(j-\tau_{\text{had}})$ in the $tt \to bb\ell\tau_{\text{had}}$ candidate event sample. The event selection requirement on this quantity has not been applied. The upper plot shows events in which the τ_{had} candidate originates from a genuine τ decay and the lower plot shows events in which the τ_{had} candidate originates from a misidentified hadronic jet

2.3.3 $Z/\gamma^* \to \tau\tau$ candidate event selection criteria

In addition to the relevant criteria on leptons given in Sect. 2.3.1 above, all candidate $Z/\gamma^* \to \tau\tau$ events ($Z \to \tau\tau \to \ell\tau_{\text{had}}$ as well as $Z \to \tau\tau \to e\mu$) are required to satisfy the following criteria:

- Events should contain no b-tagged jets.
- 50 GeV $< m_3^* <$ 100 GeV.
- $\Sigma \cos\Delta\phi > -0.1$.
- $a_T <$ 60 GeV.

The relevant variables are defined below. Distributions of each variable having applied all other selection criteria are shown in Fig. 4 for $Z \to \tau\tau \to \ell\tau_{\text{had}}$ and $Z \to \tau\tau \to e\mu$.

As expected, the rejected event samples containing b-tagged jets are dominated by tt. Because the same criterion on b-tagged jets is applied in the selection of the numerator $Z \to \tau\tau \to \ell\tau_{\text{had}}$ and denominator $Z \to \tau\tau \to e\mu$ events, we expect the ratio $R(Z)$ to be largely insensitive to systematic uncertainties associated with jet reconstruction, JES, JER, and b-tagging. Requiring no b-tagged jets reduces the background in the selected $Z/\gamma^* \to \tau\tau$ event samples from tt and also W boson plus heavy flavour production in which a b-quark jet is misidentified as a prompt e, μ, or τ_{had}. It can be seen that the other selection criteria reject a large fraction of the remaining background, principally from W+jet production (in the $Z \to \tau\tau \to \ell\tau_{\text{had}}$ sample) and from tt and diboson production (in the $Z \to \tau\tau \to e\mu$ sample).

We propose here a novel selection variable, m_3^*:

$$m_3^* \equiv \frac{m_T(\ell, \tau_{\text{had}}, \not{E}_T)}{\sin\theta_\eta^*}. \tag{12}$$

Here $\not{E}_T$ is the missing transverse momentum and the transverse mass, $m_T(\ell, \tau_{\text{had}}, \not{E}_T)$, of the 3-body system of ℓ, τ_{had}, and $\not{E}_T$ may be defined by:

$$m_T(\ell, \tau_{\text{had}}, \not{E}_T)^2 = m_T(\ell, \tau_{\text{had}})^2 + m_T(\ell, \not{E}_T)^2 + m_T(\tau_{\text{had}}, \not{E}_T)^2 \tag{13}$$

θ_η^* is an approximation to the scattering angle of the leptons relative to the beam direction in the dilepton rest frame. This variable is defined [66] solely using the measured track directions by:

$$\cos(\theta_\eta^*) \equiv \tanh\left(\frac{\eta^- - \eta^+}{2}\right), \tag{14}$$

where η^- and η^+ are the pseudorapidities of the negatively and positively charge lepton, respectively. The division by $\sin\theta_\eta^*$ in the definition of m_3^* takes into account the relative longitudinal motion of the two leptons and, therefore, m_3^* is a more closely correlated with the $\tau^+\tau^-$ mass than is $m_T(\ell, \tau_{\text{had}}, \not{E}_T)$. In the selection of $Z/\gamma^* \to \tau\tau$ candidates this improves the discrimination power against the dominant backgrounds (such as W+jet and diboson events). A comparison of the performance of m_3^* with other similar discriminating variables is shown in Fig. 5.

The variable $\Sigma\cos\Delta\phi$ [67]:

$$\Sigma\cos\Delta\phi \equiv \cos(\Delta\phi(\ell, \not{E}_T)) + \cos(\Delta\phi(\tau_{\text{had}}, \not{E}_T)), \tag{15}$$

discriminates against background events containing leptonically decaying W bosons. Here $\Delta\phi(\ell, \not{E}_T)$ is the azimuthal angle between the ℓ and the $\not{E}_T$ and $\Delta\phi(\tau_{\text{had}}, \not{E}_T)$ is the azimuthal angle between the τ_{had} and the $\not{E}_T$.

The variable a_T [68] corresponds to the component of the p_T of the dilepton system that is transverse to the dilepton thrust axis. This variable is well suited to the study of $\tau^+\tau^-$ final states, because it is less sensitive to any imbalance in the transverse momenta of the neutrinos produced in the tau decays than is a_L [68], the component of the dilepton p_T

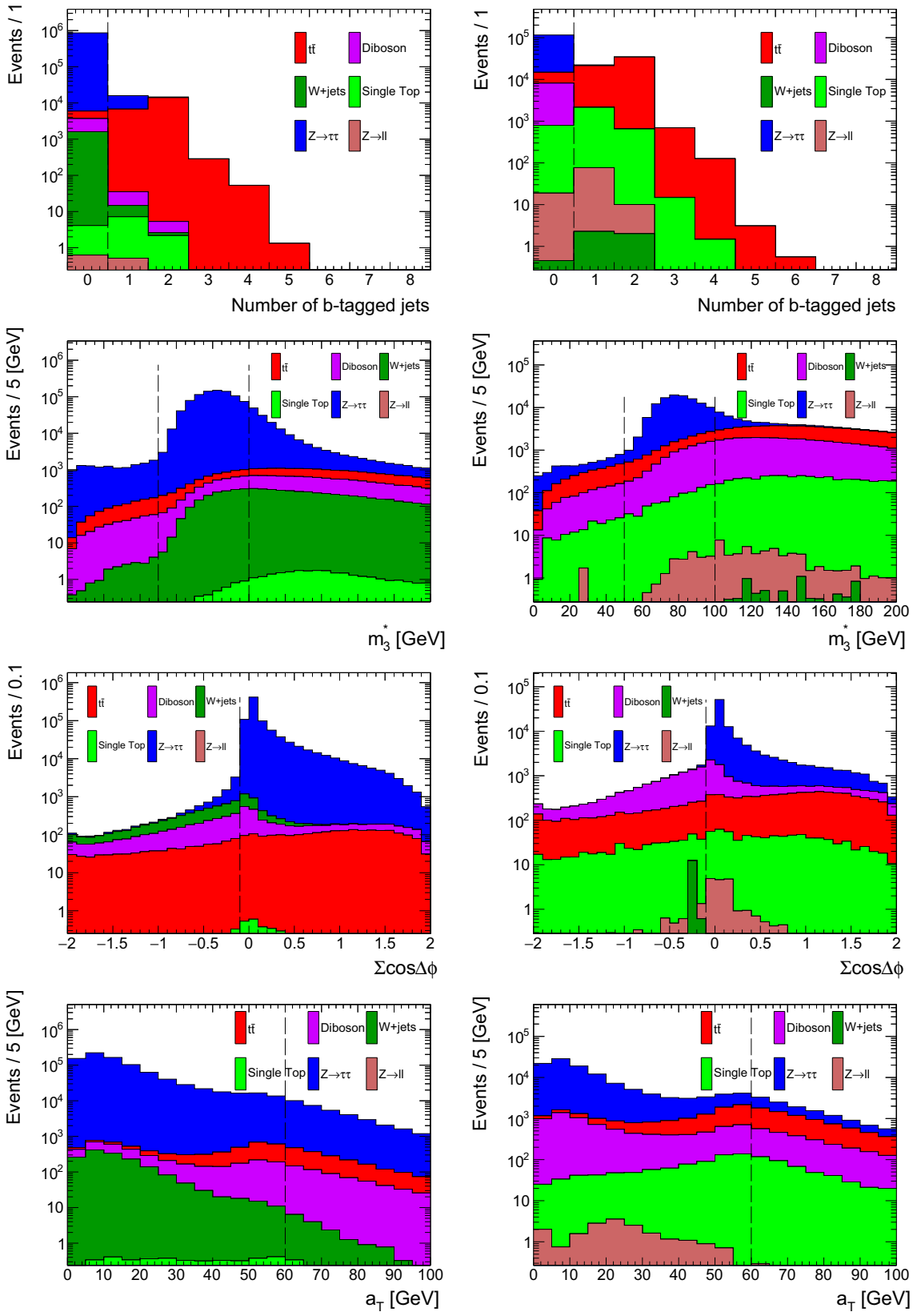

Fig. 4 Distributions of variables in the selection of $Z/\gamma^* \to \tau\tau$ candidate events having applied all other selection criteria. The left column shows $Z \to \tau\tau \to \ell\tau_{\text{had}}$ candidate events. The right column shows $Z \to \tau\tau \to e\mu$ candidate events. The selection criteria are indicated by vertical lines

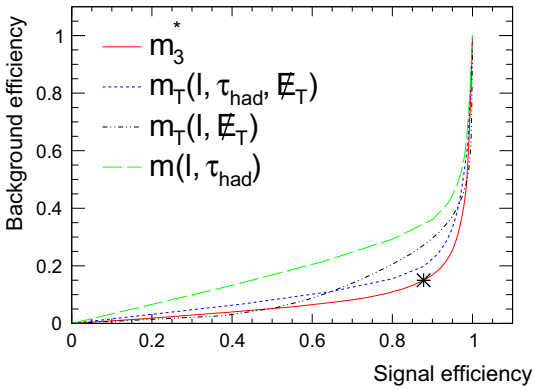

Fig. 5 A comparison of the signal and background efficiencies for cuts on different mass variables in the $Z \to \tau\tau \to \ell\tau_{\text{had}}$ candidate event sample. The variable $m(\ell, \tau_{\text{had}})$ is defined as the visible mass of the lepton and τ_{had} candidate. The star indicates the position of the proposed cut on m_3^*, which outperforms the other variables over the range of interest

that is longitudinal to the dilepton thrust axis. The variable a_T discriminates against background events containing leptonically decaying W bosons.

Figure 6 shows the distributions of p_T and $|\eta|$ of e, μ, and τ_{had}, in the selected $t\bar{t} \to b\bar{b}W^+W^-$ (red) and $Z/\gamma^* \to \tau\tau$ (blue) candidate event samples. It can be seen that the p_T distributions are considerably softer for the $Z/\gamma^* \to \tau\tau$ candidate event samples than those for the selected $t\bar{t} \to b\bar{b}W^+W^-$ candidate event samples.

As can be seen from the lower plots in Fig. 4, a cut of $a_T < 30$ GeV would be desirable to improve the suppression of backgrounds from tt and EW diboson events. However, a cut on a_T suppresses also $Z/\gamma^* \to \tau\tau$ events that contain initial state parton radiation. Initial state radiation broadens the distributions of lepton candidate p_T in $Z/\gamma^* \to \tau\tau$ events. A hard cut on a_T would therefore suppress the high-p_T regions in the distributions of lepton p_T in the selected $Z/\gamma^* \to \tau\tau$ event samples, as is illustrated in Fig. 7. The cut $a_T < 60$ GeV is chosen to reject background events from tt and diboson events, without unduly biasing the lepton p_T distributions and further accentuating the differences between the lepton p_T distributions seen in Fig. 6.

2.4 Size and composition of the selected event samples

The expected numbers of selected events and the composition of the four selected event samples for $\int L\, dt = 140$ fb^{-1} at $\sqrt{s} = 13$ TeV are given in Table 3.

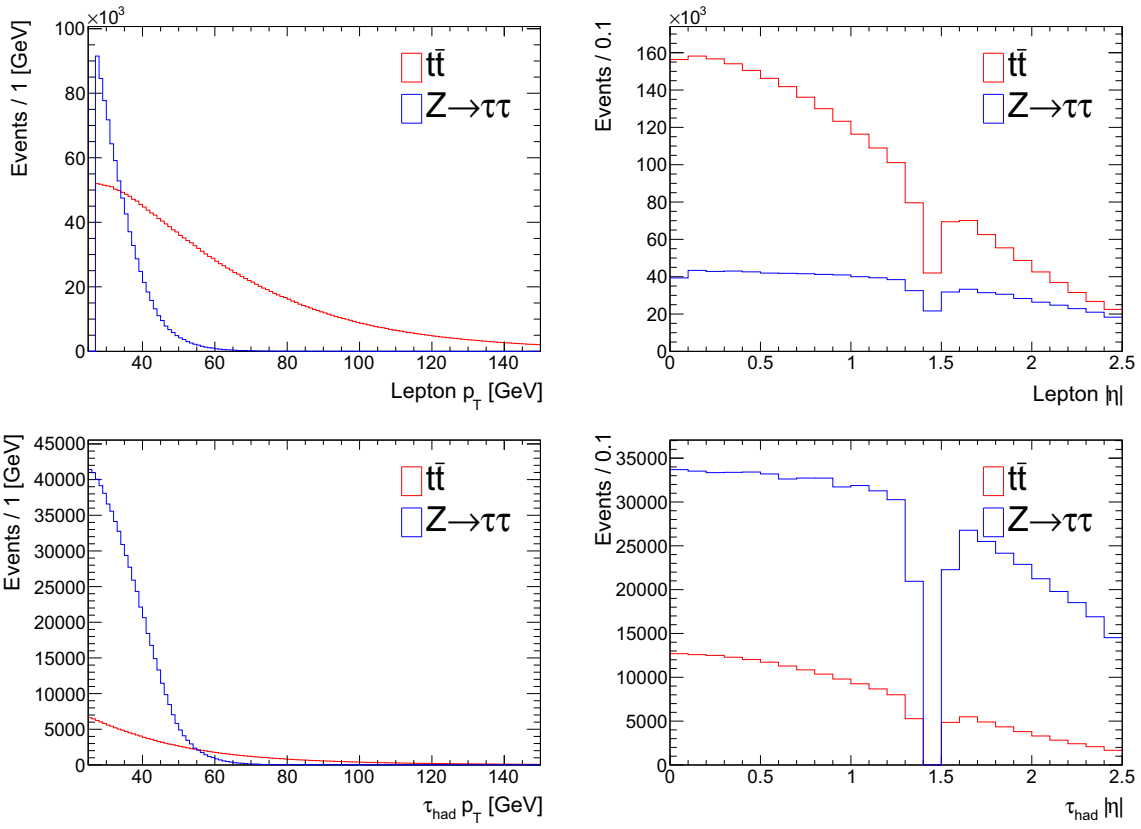

Fig. 6 The distributions of p_T and $|\eta|$ of e, μ, and τ_{had} in the selected $t\bar{t} \to b\bar{b}W^+W^-$ and $Z/\gamma^* \to \tau\tau$ candidate event samples. The left column shows p_T and the right column shows $|\eta|$. The top row shows e and μ candidates. The bottom row shows τ_{had} candidates

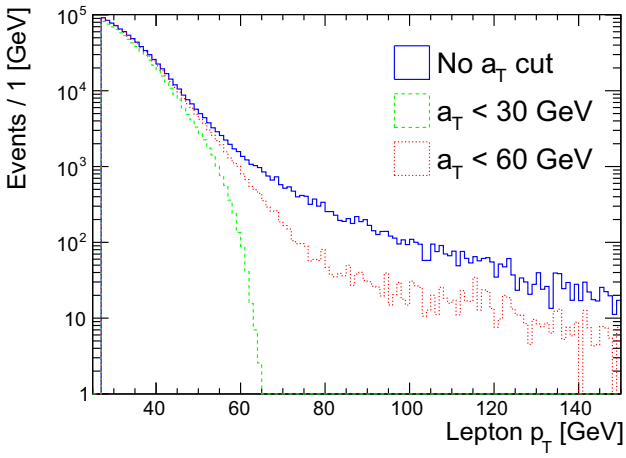

Fig. 7 Distributions of lepton p_T in the selected $Z/\gamma^* \to \tau\tau$ candidate event samples. Three different cuts on a_T are applied

As a result of this study we estimate that the fractional statistical uncertainty on $R(WZ)$ for a single LHC experiment for an integrated luminosity of $\int L\,\mathrm{d}t = 140\ \mathrm{fb}^{-1}$ would be around 0.5%.

The selection requirements for $tt \to bb\ell\tau_{\mathrm{had}}$ and $tt \to bbe\mu$ can be seen to be very effective at removing non-tt sources of background, e.g., W+jet. The most significant source of non-tt events originates from the EW production of "single top" events in the associated production tWb channel. Since these events contain two genuine leptonically decaying W bosons they can effectively be considered as contributing to the signal sample, and not as background. They are listed as "tWb true" in Table 3. Single top processes that do not contain a pair of W bosons decaying to produce two correctly identified leptons are classified as background. Events which contain the associated production of either a W or Z boson with a tt pair ($t\bar{t}V$) can be considered signal if they contain at least two W bosons which decay to correctly identified leptons. Since the fractions of these events are small, $< 0.1\%$, they are included in the tt categories in Table 3.

The most significant source of background for $tt \to bb\ell\tau_{\mathrm{had}}$ originates from genuine tt events in which the τ_{had} candidate originates from a misidentified hadronic jet. The residual background from this source corresponds to about 2.5% of the selected sample of candidate $tt \to bb\ell\tau_{\mathrm{had}}$ events. The $tt \to bbe\mu$ candidate event sample will be selected with entirely negligible levels of background.

The most significant source of background for $Z \to \tau\tau \to \ell\tau_{\mathrm{had}}$ originates from QCD *multijet* (MJ) events (that is, events that do not contain any prompt leptons from W or Z boson decay). This background is estimated to be at the level of around 5%, as described in the Appendix and [44]. In comparison, the MC-estimated backgrounds for $Z \to \tau\tau \to \ell\tau_{\mathrm{had}}$ from tt (0.3%) and W+jet (0.2%) are small. The most significant sources of background for $Z \to \tau\tau \to e\mu$ originate from tt (5.8%) and diboson (6.3%) production.

2.5 Sensitivity of $R(WZ)$ to $R(W)$

For definiteness we make the assumption in our study that the effective $W \to \tau\nu$ coupling relevant for on-mass-shell W boson decays could be modified by some BSM effect, whilst all other W boson couplings are maintained at their

Table 3 The expected numbers of events in the four selected event samples for $\int L\,\mathrm{d}t = 140\ \mathrm{fb}^{-1}$ at $\sqrt{s} = 13$ TeV. The numbers are broken down by physics production process. The numbers for tt, single top and Z boson production are further broken down into the two categories "true", in which the two lepton candidates are correctly identified, and "fake", in which at least one of the lepton candidates is incorrectly identified. Small numbers of events from $t\bar{t}V$ processes that contain two correctly identified leptonic W boson decays are included in the tt "true' category. Otherwise, the events from $t\bar{t}V$ processes are included in the tt "fake" category. The numbers given in **bold** type represent the signal in the four selected event samples. The numbers given under "Total background" include the "fake" categories described above

Process	Selected event sample			
	$tt \to bb\ell\tau_{\mathrm{had}}$	$tt \to bbe\mu$	$Z \to \tau\tau \to \ell\tau_{\mathrm{had}}$	$Z \to \tau\tau \to e\mu$
$t\bar{t} \to b\bar{b}W^+W^-$ true	**178270**	**1092395**	2034	6517
$t\bar{t} \to b\bar{b}W^+W^-$ fake	4761	0	20	156
tWb true	**3236**	**18209**	0	725
tWb fake	74	0	1	8
Other single top	1731	0	2	42
$Z/\gamma^* \to \tau\tau$ true	3	256	**657280**	**101074**
$Z \to ee, \mu\mu, \tau\tau$ fake	0	0	1	14
W+jets	61	0	1226	0
WW true	27	166	1555	6580
Other diboson	5	25	337	773
Total background	6663	447	5176	14815

SM-predicted values. Under this assumption, if the branching ratio $\mathcal{B}(W \to \tau\nu)$ is multiplied by a factor X relative to its SM-predicted value $\mathcal{B}(W \to \tau\nu)_{\mathrm{SM}}$,

$$\mathcal{B}(W \to \tau\nu) = X.\mathcal{B}(W \to \tau\nu)_{\mathrm{SM}} \tag{16}$$

then all other W boson branching fractions will be modified by a factor

$$F = \frac{1 - X.\mathcal{B}(W \to \tau\nu)_{\mathrm{SM}}}{1 - \mathcal{B}(W \to \tau\nu)_{\mathrm{SM}}}. \tag{17}$$

In our MC study we perform a "calibration" of the double-ratio method by reweighting every simulated event containing one or more W boson decays by a factor $X^n F^m$, where n is the number of generator-level $W \to \tau\nu$ decays and m is the number of other W boson decays. This calibration procedure properly takes into account all events in the calculation of $R(bbWW)$ that contain pairs of leptonically decaying W bosons with correctly identified decay products in the "numerator" $tt \to bb\ell\tau_{\mathrm{had}}$ and "denominator" $tt \to bbe\mu$ samples. This includes, for example, the presence of events containing the cascade decay $W \to \tau\nu \to \ell\nu\nu$, whose presence in the "denominator" $tt \to bbe\mu$ sample slightly decreases the correlation between $R(bbWW)$ and $R(W)$. The value of $R(Z)$ is designed to be independent of any change in $R(W)$. However, the backgrounds from $t\bar{t} \to b\bar{b}W^+W^-$ and WW in the $Z \to \tau\tau \to \ell\tau_{\mathrm{had}}$ and $Z \to \tau\tau \to e\mu$ events contain decays of W bosons, which cause the expected background levels to alter with $R(W)$. A correction to the $R(Z)$ calculation from this effect is included. The result of this calibration is shown in Fig. 8, which shows the fractional change in $R(bbWW)$, $R(Z)$, and $R(WZ)$ as a function of the fractional change in $R(W)$. The absolute value of the ratio of $R(W)$ and $R(WZ)$ will depend on the precise experimental details specific to a given experiment and would have to be evaluated using fully simulated MC events for the specific identification criteria and event selection cuts employed in the analysis of the experimental data.

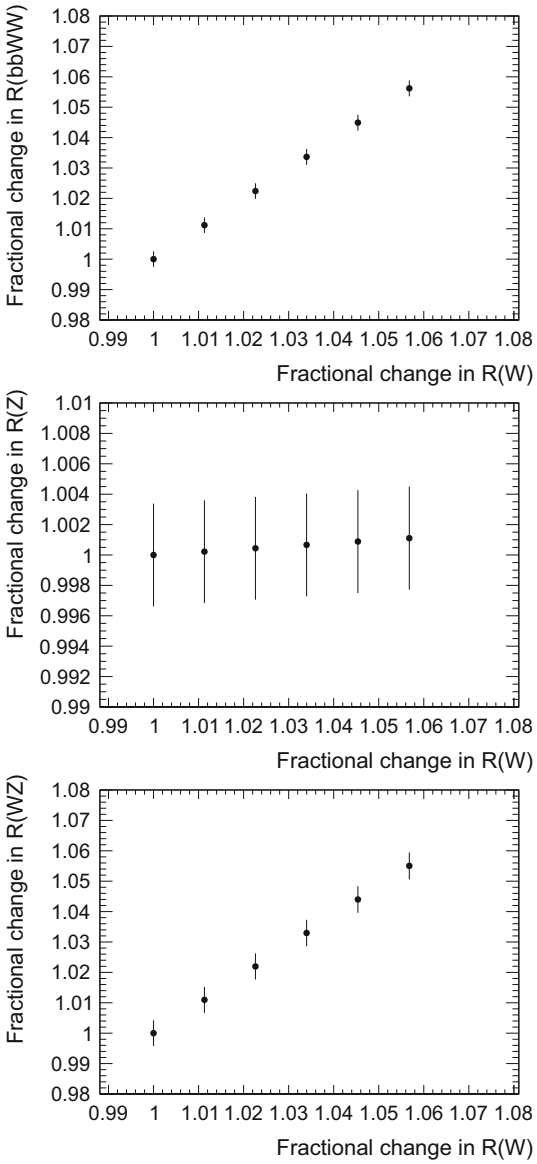

Fig. 8 The fractional change in $R(bbWW)$ (upper), $R(Z)$ (middle), and $R(WZ)$ (lower), as a function of the fractional change in $R(W)$, obtained by reweighting events at generator level as described in the text. The displayed error bars illustrate the expected experimental statistical uncertainty on the relevant quantity, and are completely correlated point to point. MC statistical uncertainties on the point-to-point variation with $R(W)$ are negligible

2.6 Evaluation of systematic uncertainties

Considering each source of systematic uncertainty described in Sects. 2.1 and 2.2, and summarised in Tables 1 and 2, we evaluate the resulting changes in the ratios $R(bbWW)$, $R(Z)$, $R(WZ)$, and $R(W)$.

The p_T/η-independent and p_T/η-dependent systematic variations on the reconstruction of leptons and jets, as summarised in Table 1, are considered separately. The resultant changes in the ratios are given in Table 4. It can be seen that the p_T/η-independent systematic uncertainties on $R(bbWW)$ and $R(Z)$ are large, but almost exactly equal. Therefore, p_T/η-independent systematic uncertainties on the reconstruction of leptons and jets almost perfectly cancel in the double ratio $R(WZ)$. When considering p_T/η-dependent systematic uncertainties the cancellation is no longer perfect. The most significant sources of p_T/η-dependent systematic uncertainties are illustrated in Fig. 9. The 10% uncertainty on the 2.5% background from hadronic jets misidentified as τ_{had} candidates in the $tt \to bb\ell\tau_{\mathrm{had}}$ sample leads to an uncertainty of 0.25% on $R(bbWW)$ and thus also on $R(W)$. The 5% uncertainty on the 5% background from MJ events in the $Z \to \tau\tau \to \ell\tau_{\mathrm{had}}$ sample leads to an uncertainty of

Table 4 Changes in the ratios $R(bbWW)$, $R(Z)$, and $R(WZ)$ resulting from the sources of experimental systematic uncertainty described in Sect. 2.1 and summarised in Table 1. The p_T/η-independent and p_T/η-dependent systematic variations are considered separately

Source of	Systematic uncertainty on measured ratios (%)					
Systematic	p_T/η-independent variation			p_T/η-dependent variation		
Uncertainty	$R(bbWW)$	$R(Z)$	$R(WZ)$	$R(bbWW)$	$R(Z)$	$R(WZ)$
Tau ID	5.0	5.0	< 0.1	3.9	4.7	0.8
Electron ID	1.1	1.3	0.2	0.5	1.2	0.7
Electron trigger	0.3	0.2	0.1	0.1	0.3	0.2
Muon trigger	0.4	0.5	0.1	0.4	0.5	0.1
Muon ID	1.0	0.7	0.3	0.1	0.2	< 0.1
b-jet ID	< 0.1	< 0.1	< 0.1	–	–	–
Light jet mis-ID	0.1	0.1	< 0.1	–	–	–
Tau p_T scale	< 0.1	< 0.1	< 0.1	< 0.1	< 0.1	< 0.1
Electron p_T scale	< 0.1	< 0.1	< 0.1	< 0.1	< 0.1	< 0.1
Muon p_T scale	< 0.1	< 0.1	< 0.1	< 0.1	< 0.1	< 0.1
Jet energy scale	< 0.1	< 0.1	< 0.1	–	–	–
Electron p_T resolution	< 0.1	< 0.1	< 0.1	< 0.1	< 0.1	< 0.1
Muon p_T resolution	< 0.1	< 0.1	< 0.1	< 0.1	< 0.1	< 0.1
Fake τ_{had} background ($tt \to bb\ell\tau_{\text{had}}$ sample)	0.25	0	0.25	–	–	–
MJ background ($Z \to \tau\tau \to \ell\tau_{\text{had}}$ sample)	0	0.25	0.25	–	–	–

0.25% on $R(Z)$ and thus also on $R(W)$. Since the above two backgrounds both result from hadronic jets misidentified as τ_{had} candidates it is conceivable that the resultant systematic uncertainties on $R(bbWW)$ and $R(Z)$ could be correlated and thus partially cancel in the calculation of $R(W)$. A realistic estimate of the degree of correlation will depend on experimental details beyond the scope of the current study and we have not taken into account any potential reduction in the systematic uncertainty on $R(W)$.

The sources of phenomenological systematic uncertainty considered in this study are summarised in Table 2 and the resultant changes in the ratios $R(bbWW)$, $R(Z)$, and $R(WZ)$ are given in Table 5. The 3% uncertainty on the backgrounds from tt (5.8%) and diboson (6.3%) production in the $Z \to \tau\tau \to e\mu$ sample leads to uncertainties of 0.2% and 0.2%, respectively, on $R(Z)$ and thus also on $R(W)$. The uncertainty resulting from the $p_T(Z)$ reweighting procedure is <0.1% on $R(Z)$, and thus also on $R(W)$.

The alternative tt sample with modified QCD factorisation and renormalisation scales leads to an uncertainty of 0.3% on $R(bbWW)$ and thus also on $R(W)$ [69]. The $m(t\bar{t})$ reweighting leads to an uncertainty of 0.2% on $R(bbWW)$ and thus also on $R(W)$.

We add in quadrature the changes in the double ratio $R(WZ)$ arising from the p_T/η-independent and p_T/η-dependent systematic variations on the reconstruction of leptons and jets, together with the other considered systematic uncertainties discussed above. The total resulting systematic uncertainty on $R(WZ)$ is 1.3%.

2.7 Considerations for future measurements

Measurements of $R(W)$ on the data from ATLAS and CMS using the double ratio technique proposed here will, clearly, require the use of fully simulated MC events and will employ the sophisticated procedures developed by the individual experiments to evaluate backgrounds and experimental systematic uncertainties. Our study is based on particle-level MC events and a simple parameterised simulation of detector performance. Nevertheless, we believe our demonstration that the dominant experimental systematic uncertainties cancel in the double ratio, as well as our estimates of the major residual systematic uncertainties, to be broadly realistic. We have based our simulation of lepton, jet and $\not{E}_T$ reconstruction on measurements of efficiencies, backgrounds and systematic uncertainties published by ATLAS and CMS [24–55], having chosen identification algorithms whose performance is suited to the needs of our analysis. The above cited performance papers are for the most part based on around a quarter of the full run 2 data set of $\int L\, \mathrm{d}t = 140\,\mathrm{fb}^{-1}$ at $\sqrt{s} = 13\,\mathrm{TeV}$ that is now available. It is, therefore, to be expected that the full run 2 data set will allow systematic uncertainties on lep-

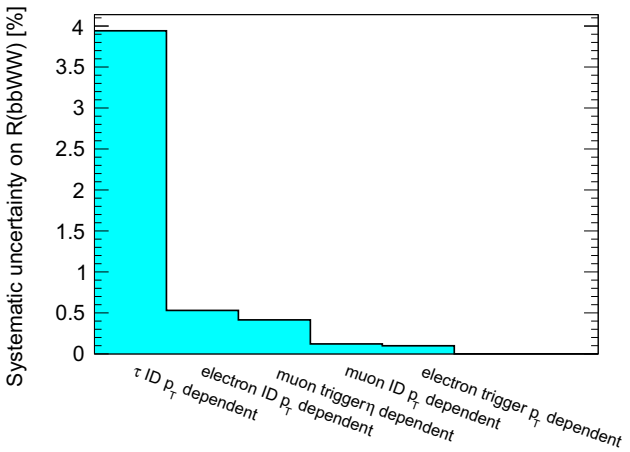

(a) $R(bbWW)$

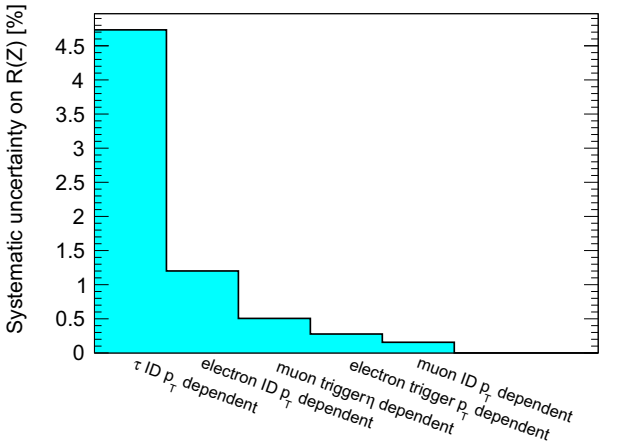

(b) $R(Z)$

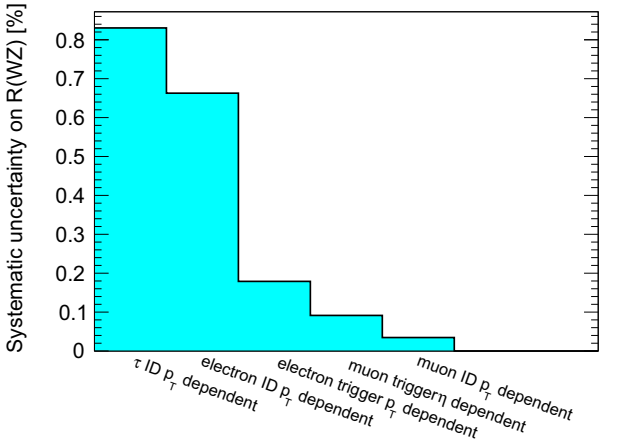

(c) $R(WZ)$

Fig. 9 Summary of the most significant changes in the ratios **a** $R(bbWW)$, **b** $R(Z)$, and **c** $R(WZ)$ arising from sources of p_T/η-dependent systematic uncertainty. From left to right in each sub-figure the sources are ordered in descending magnitude of the resulting systematic uncertainty

Table 5 Changes in the ratios $R(bbWW)$, $R(Z)$, and $R(WZ)$ resulting from the sources of phenomenological systematic uncertainty described in Sect. 2.2 and summarised in Table 2

Source of systematic uncertainty	Systematic uncertainty on measured ratios (%)		
	$R(bbWW)$	$R(Z)$	$R(WZ)$
tt background in $Z \to \tau\tau \to e\mu$ sample	0	0.2	0.2
Diboson background in $Z \to \tau\tau \to e\mu$ sample	0	0.2	0.2
$p_T(Z)$ reweighting	0	< 0.1	< 0.1
$m(t\bar{t})$ reweighting	0.2	0	0.2
tt modelling	0.3	0	0.3

ton and jet identification efficiencies to be reduced by about a factor of two compared to the values we have assumed in our study. Of particular relevance to our study, it is to be hoped that the high statistics provided by the full run 2 data set will allow the p_T dependence of the identification efficiency for τ_{had} candidates to be studied over the range $25 < p_T < 100$ GeV, without the need to use $tt \to bb\ell\tau_{\text{had}}$ events and implicitly assume that $\mathcal{B}(W \to \tau\nu)$ takes its SM value. This could be achieved, e.g., by the selection of a dedicated $Z \to \tau\tau \to \ell\tau_{\text{had}}$ event sample in which there is a high transverse momentum initial state radiation.

The residual non-cancellation in $R(WZ)$ of the p_T/η-dependent τ_{had} identification uncertainty, as shown in Table 4, arises primarily from the differences in the τ_{had} p_T distributions between the $tt \to bb\ell\tau_{\text{had}}$ and $Z \to \tau\tau \to \ell\tau_{\text{had}}$ samples, as shown in Fig. 6. We have considered possible methods to reduce the impact of the different τ p_T distributions. One simple approach would be to introduce an additional cut on τ_{had} $p_T < 65$ GeV; this removes the high p_T tail in the $tt \to bb\ell\tau_{\text{had}}$ sample, with negligible changes to the $Z \to \tau\tau \to \ell\tau_{\text{had}}$ sample. This has the effect of improving the cancellation in $R(WZ)$ of the p_T-dependent τ_{had} identification uncertainty between the $tt \to bb\ell\tau_{\text{had}}$ and $Z \to \tau\tau \to \ell\tau_{\text{had}}$ samples; the residual systematic uncertainty reduces from 0.8%, as shown in Table 4, to 0.2%. More sophisticated potential methods to mitigate the effects of the p_T-dependent τ_{had} identification uncertainty might be (a) to reweight the tau p_T distribution in the $tt \to bb\ell\tau_{\text{had}}$ sample to resemble that in the $Z \to \tau\tau \to \ell\tau_{\text{had}}$ sample, or (b) to perform measurements of $R(WZ)$ in bins of τ_{had} p_T and subsequently combine the measurements, taking into account the bin-to-bin correlations in the systematic uncertainties. However, any such methods might run the risk of increasing the sensitivity of $R(WZ)$ to phenomenological uncertainties. A careful investigation of such issues will be needed in order to optimise the overall uncertainty arising

from experimental and phenomenological systematic uncertainties. This will require study of the large number of fully simulated MC samples produced by the experiments, corresponding to different models of tt and Z boson production and decay, and is beyond the scope of this paper.

Of course, if the measured value of $R(WZ)$ is found to disagree with that expected in the SM then further studies will be required to ascertain the nature of BSM physics that is responsible. For example, the decay $t \to bH^+$, where H^+ is a charged higgs boson, followed by $H^+ \to \tau^+\nu$ would modify the effective $t \to b\tau\nu$ and $t \to b\ell\nu$ branching ratios in a similar fashion to that discussed in the context of equations 16 and 17 above. Similarly, top decays via a neutral higgs boson $t \to qH$, $H \to \tau\tau$ will also increase the number of tau leptons in tt events relative to the SM-expected value. Existing experimental searches for charged [70,71] and neutral [72] higgs bosons in top quark events suffer from the large systematic uncertainties associated with τ_{had} identification and will benefit from the double ratio method we propose in this paper to reduce experimental systematic uncertainties.

The large numbers of events from the EW production of diboson events (WW and WZ) at the LHC provide alternative samples with which to make this novel measurement. Controlling systematic uncertainties on $R(W)$ in $WW \to \ell\nu\tau_{\text{had}}\nu$ events will be extremely challenging; we shall need extraordinarily good background rejection against fake τ candidates from misidentified jets in $W \to \ell\nu$+ jet events. One may also consider $ZW \to \ell\ell\tau_{\text{had}}\nu$ as an alternative sample with which to perform this measurement. This channel provides lower statistics because of the lower cross section times branching fraction. However, one can veto on Z+jet backgrounds by removing events in which the $\ell^+\ell^-$ momentum is back to back with the τ candidate direction. One can calibrate the residual backgrounds by looking at the back-to-back events. If the experimental measurements proposed here observe a clear violation of LU then having three channels $tt \to bb\ell\tau_{\text{had}}$, $WW \to \ell\nu\tau_{\text{had}}\nu$, and $ZW \to \ell\ell\tau_{\text{had}}\nu$ could increase the significance of the observation, and could help elucidate the underlying BSM origin of the effect.

In addition to the $tt \to bb\ell\tau_{\text{had}}$ and $Z \to \tau\tau \to \ell\tau_{\text{had}}$ final states considered here, it may be possible to measure $R(W)$ using a similarly motivated ratio of $tt \to bb\ell\tau_{\text{lept}}$ and $Z \to \tau\tau \to \ell\tau_{\text{lept}}$ final states, where τ_{lept} corresponds to a leptonic decay of the τ, that may be identified using, for example, criteria based on the non-zero lifetime of the τ lepton. A combination of $R(W)$ measurements using τ_{had} and τ_{lept} signatures would benefit from the fact that the leading experimental uncertainties, arising from τ_{had} and τ_{lept} identification, would be largely uncorrelated.

3 Summary and conclusions

A measurement of $R(W) \equiv \mathcal{B}(W \to \tau\nu)/\mathcal{B}(W \to \ell\nu)$ ($\ell = e$ or μ) represents a promising opportunity to discover a violation of lepton universality. We propose here a novel double-ratio method that will allow $R(W)$ to be measured using top quark pairs and $Z/\gamma^* \to \tau\tau$ events at the LHC.

We define $R(bbWW)$ in di-leptonic tt events to be the ratio of the numbers of $\ell\tau_{\text{had}}$ and $e\mu$ final states (equation 9). $R(bbWW)$ is sensitive to the value of $R(W)$, but also to systematic uncertainties on the reconstruction of e, μ, and τ leptons. Similarly, we define $R(Z)$ in $Z/\gamma^* \to \tau\tau$ events to be the ratio of the numbers of $\ell\tau_{\text{had}}$ and $e\mu$ final states (equation 10). $R(Z)$ is similarly sensitive to systematic uncertainties on the reconstruction of e, μ, and τ leptons, but is insensitive to the value of $R(W)$. The double ratio $R(WZ) \equiv R(bbWW)/R(Z)$ cancels to first order sensitivity to systematic uncertainties on the reconstruction of e, μ, and τ leptons, thus improving very significantly the precision to which $R(W)$ can be measured at a hadron collider

We have performed a study of the double ratio $R(WZ)$ using particle-level MC events and a parameterised simulation of detector performance. We have based our simulation of lepton, jet and $\not{E}_T$ reconstruction on measurements of efficiencies, backgrounds and systematic uncertainties published by ATLAS and CMS [24–55], having chosen identification algorithms whose performance is suited to the needs of our analysis. For a data set of $\int L\, \mathrm{d}t = 140\ \mathrm{fb}^{-1}$ at $\sqrt{s} = 13$ TeV we estimate a statistical uncertainty on $R(W)$ of 0.5%. Our study confirms the almost perfect cancellation in $R(W)$ of systematic uncertainties on the reconstruction efficiencies of e, μ, and τ leptons that are applied as constant factors. We find that the most significant residual sources of uncertainty on $R(W)$ arise from systematic uncertainties on the p_T and η dependence of the reconstruction efficiencies of e, μ, and τ leptons, which total around 1.0%. We have evaluated also potential uncertainties arising from backgrounds to the selected event samples and from various phenomenological sources.

Our studies indicate that a single experiment precision on the measurement of $R(W)$ of around 1.4% is achievable with a data set of $\int L\, \mathrm{d}t = 140\ \mathrm{fb}^{-1}$ at $\sqrt{s} = 13$ TeV. This would improve significantly upon the precision of the LEP2 measurements of $R(W)$. If the central value of the new measurements were equal to the central value of the LEP2 measurements this would yield an observation of BSM physics at a significance level of around 5σ.

Acknowledgements Final year undergraduate (MPhys) project students working in Manchester with T.W. have made some important contributions to the ideas presented in this paper. Jihyun Jeong (1993–2018) and Robin Upham made an early feasibility study for the measurement of $R(bbWW)$ using tt events at the LHC. Vilius Cepaitis and Ricardo Wölker studied possible improvements to the selection of

$Z/\gamma^* \to \tau\tau$ events at the LHC from which the variable m_3^* arose. We are very grateful to our colleague Chris Parkes for his useful suggestions for the improvement of this paper.

Data Availability Statement This manuscript has no associated data or the data will not be deposited. [Authors' comment: It presents a feasibility study using generator-level MC events with parameterised simulation of detector performance. All experimental data is taken from published sources.]

Funded by SCOAP[3].

Appendix: Detailed description of the parameterised detector simulation

We give here a detailed description of our choices of lepton and jet identification algorithms to simulate, the experimental systematic uncertainties we consider, and the reasoning behind these choices.

A.1 Simulation of muon candidates

The efficiencies and systematic uncertainties associated with the reconstruction and identification of high p_T, isolated muon candidates have been presented by the ATLAS [24] and CMS [25] collaborations. In both experiments the muon reconstruction efficiency is around 99% and is independent of p_T and $|\eta|$, except for some well-defined, poorly instrumented regions of both detectors that are usually excluded for precision measurements. We choose to simulate the efficiency for muon identification according to that given for the "Medium" category described in [24]. This gives an efficiency of around 96% for muons with $p_T > 20$ GeV. Systematic uncertainties on the efficiency are around 0.1% for muon p_T around $m_Z/2$, increasing to around 0.5% for $p_T \approx 30$ GeV and $p_T \approx 100$ GeV. We choose to simulate the "Tight" lepton isolation requirement given in [24], which is measured to have an efficiency that is independent of p_T and $|\eta|$ of around 96% with a systematic uncertainty at the per mille level. We assume the efficiency of the isolation criteria for sources of non-prompt muons to be 0.03, based on the range of values given in [24]. We consider a combined systematic uncertainty on the efficiency for muon reconstruction, identification, and isolation. We consider a p_T/η-independent relative systematic uncertainty of 2%. We generate a p_T-dependent systematic uncertainty by modifying the efficiency by a relative amount that varies linearly between 0.5% at $p_T = 30$ GeV and 0% at $p_T = 80$ GeV and above.

We simulate the efficiency of the single muon trigger to be 65% (80%) in the barrel (endcap) region, as has been measured for ATLAS [26,27]. We define the barrel region by $|\eta| < 1.0$ and the endcap region by $|\eta| > 1.0$. For offline p_T at least 1 GeV above the trigger threshold the efficiency is almost independent of p_T. The trigger threshold is assumed to be similar to the electron trigger threshold of ATLAS during most of run 2 at $p_T = 26$ GeV [28]. We consider a p_T/η-independent relative systematic uncertainty of 1%. We generate an η-dependent systematic uncertainty by modifying the relative efficiency by 1% in the endcap region, whilst the efficiency in the barrel region remains unchanged.

We simulate the resolution in muon p_T by means of a Gaussian with a width of 2.30 ± 0.15% in the barrel region and 2.90 ± 0.15% in the endcap region, independent of p_T [24]. We consider a p_T/η-independent relative systematic uncertainty of 0.2% on the p_T scale [24]. We generate η-dependent systematic uncertainties by modifying the resolution and p_T scale only in the endcap region, whilst the values in the barrel region remain unchanged.

A.2 Simulation of electron candidates

The efficiencies and systematic uncertainties associated with the reconstruction and identification of high p_T, isolated electron candidates have been presented by the ATLAS [29] and CMS [30] collaborations. In both experiments the electron reconstruction efficiency is around 98% and is fairly independent of p_T and $|\eta|$, except for some well-defined, poorly instrumented regions of both detectors [31]. A general feature in both ATLAS and CMS is that the efficiency of the commonly used electron identification algorithms tend to have a larger dependence on p_T than is the case for muon identification. We choose to simulate approximately the efficiency for electron identification according to the "Tight likelihood" algorithm of [29]. The efficiency is around 75% at $p_T = 30$ GeV and rises to around 90% for $p_T > 80$ GeV and above [32]. The efficiency is determined with a systematic uncertainty of a few per mille for $p_T > 30$ GeV. We choose to simulate also for electrons the "Tight" lepton isolation requirement given in [24], with an efficiency that is independent of p_T and $|\eta|$ of around 96%. We consider a combined systematic uncertainty on the efficiency for electron reconstruction, identification, and isolation. We consider a p_T/η-independent relative systematic uncertainty of 2%. We generate a p_T-dependent systematic uncertainty by modifying the efficiency by a relative amount that varies linearly

between 2% at $p_T = 30$ GeV and 0% at $p_T = 80$ GeV and above.

The efficiency of the single electron trigger has been measured in ATLAS to be around 90% for offline p_T at least 1 GeV above the trigger threshold [33]. We consider a p_T/η-independent relative systematic uncertainty of 1%. We generate a p_T-dependent systematic uncertainty by modifying the position of the effective trigger threshold in p_T by 1 GeV.

The resolution and p_T scale for high p_T, isolated electron candidates and the associated systematic uncertainties have been measured by the ATLAS [34] and CMS [30] collaborations. We simulate the resolution in electron p_T by means of a Gaussian with a width σ_{p_T} given by $\frac{\sigma_{p_T}}{p_T} = \frac{0.16}{\sqrt{p_T}}$. We consider a p_T/η-independent systematic uncertainty on the resolution by varying the constant term in the formula for $\frac{\sigma_{p_T}}{p_T}$ by an amount ± 0.002 [35]. The p_T scale is calibrated with a precision of around 0.2% in both ATLAS and CMS [30,34]. We consider a p_T/η-independent relative systematic uncertainty of 0.2% on the p_T scale. We generate η-dependent systematic uncertainties by modifying the resolution and p_T scale only in the endcap region, whilst the values in the barrel region remain unchanged.

Since we apply tight isolation requirements on the candidate leptons, we make the conservative assumption that the identification efficiency for non-prompt electrons from heavy flavour decays is the same as that for prompt electrons. In [36] around 2/3 of the background electrons arise from heavy flavour decays. The remaining background arises from photon conversions and misidentified hadrons, which are difficult to simulate in the context of our parameterised detector simulation. We therefore make the approximation that the total background to the sample of high p_T, isolated electrons in the simulated events is obtained by multiplying the number of electrons from heavy flavour decays by a factor of 1.5.

A.3 Simulation of τ_{had} candidates

Of central importance to any measurement of $R(W)$ at a hadron collider will be an understanding of the efficiencies and backgrounds associated with the identification of τ candidates. A recent paper by the CMS Collaboration [37] describes the methods used to identify τ_{had} candidates at $\sqrt{s} = 13$TeV and details the methods used to determine identification efficiencies, background rates and energy scale, and their associated systematic uncertainties, using a data set corresponding to $\int L\, \mathrm{d}t = 36\ \mathrm{fb}^{-1}$. We choose to simulate the τ_{had} identification efficiency and fake probabilities corresponding to the "very-very-tight" operating point of [37]. The efficiency is around 30% and is independent of p_T. The misidentification rate for hadronic jets is around 2×10^{-3} for $p_T \approx 25$ GeV decreasing to around 10^{-4} for $p_T \approx 100$ GeV. The misidentification rate is approximately independent of $|\eta|$ [38]. We simulate also the discriminants against electrons and muons described in [37]: the "Tight" discriminant against electrons has a τ_{had} identification efficiency of 75% and a fake probability of 10^{-3}; the "Tight" discriminant against muons has a τ_{had} identification efficiency of 99% and a fake probability of 1.4×10^{-3} [39].

In our study it is particularly important to assign realistic systematic uncertainties on the identification efficiency for τ_{had} candidates. A tag and probe analysis of $Z \to \tau\tau \to \ell\tau_{\text{had}}$ events in [37] results in a relative uncertainty on the identification efficiency of τ_{had} candidates of 5% for τ_{had} p_T up to 60 GeV. Samples of tt events are used in [37] to cross check the efficiency for τ_{had} p_T up to 100 GeV; a relative uncertainty of 7% for $60 < p_T < 100$ GeV is assigned. Implicitly this latter analysis assumes that $\mathcal{B}(W \to \tau\nu)$ takes its SM value, because it relies on a comparison between the absolute numbers of $tt \to bb\ell\tau_{\text{had}}$ candidate events observed in the CMS data and predicted by the MC. Clearly, for our proposed test of LU using tt events it would not be legitimate to set data-MC scale factors for τ_{had} using $tt \to bb\ell\tau_{\text{had}}$ events in this way; this means that it will be difficult to control the p_T dependence of the identification efficiency for τ_{had} candidates beyond the range in τ_{had} p_T covered by the $Z \to \tau\tau \to \ell\tau_{\text{had}}$ event sample. We consider a p_T/η-independent relative systematic uncertainty of 5%. We generate a p_T-dependent systematic uncertainty on the identification efficiency of τ_{had} candidates by modifying the efficiency by a relative amount that varies linearly between 5% at $p_T = 30$ GeV and 0% at $p_T = 130$ GeV and above. The p_T resolution for τ_{had} candidates is given by $\frac{\sigma_{p_T}}{p_T} = 0.16$ [40].

The relative uncertainties on the probabilities for electrons, muons, and hadronic jets to be misidentified as a τ_{had} candidate are around 10% [41]. The uncertainty on the p_T scale for τ_{had} candidates is around 1% [37]. We consider an η-dependent systematic uncertainty by modifying the p_T scale by 1% only in the endcap region, whilst the scale in the barrel region remains unchanged. Preliminary systematic uncertainties of a similar magnitude have been assessed by the ATLAS Collaboration for the identification of τ_{had} candidates at $\sqrt{s} = 13$ TeV [42], using the methods described in [43].

Backgrounds from MJ events are typically estimated at hadron colliders using data driven methods. Such backgrounds cannot reliably be estimated from MC. Of the four signal samples, $Z \to \tau\tau \to \ell\tau_{\text{had}}$ will be the sample with the largest fraction of MJ background. An important motivation for our choice to simulate the "very-very-tight" operating point of [37] for τ_{had} identification, which has relatively low efficiency but high rejection power, is to minimise the uncertainties arising from MJ backgrounds. From [25] and [37] we estimate the fraction of MJ background in the selected

$Z \to \tau\tau \to \ell\tau_{\text{had}}$ sample to be around 5%, with a relative uncertainty of around 5% [44].

The probability to mis-measure the sign of the charge of lepton candidates is expected to be less than 1% over the range of p_T of relevance to our study and is neglected in our simulation.

A.4 Simulation of hadronic jets, including b-tagging

Jet finding is performed at particle-level using the anti-k_t algorithm [45] with a distance parameter $R = 0.4$. Determinations of the jet energy scale (JES) and jet energy resolution (JER), along with their systematic uncertainties, have been presented by the ATLAS [46] and CMS [47] collaborations. We simulate the resolution in jet p_T by means of a Gaussian with a width σ_{p_T} given by $\frac{\sigma_{p_T}}{p_T} = \frac{1.0}{\sqrt{p_T}}$. We assume an uncertainty on the jet energy scale of 1%.

The efficiencies, backgrounds and systematic uncertainties associated with the b-tagging of hadronic jets have been presented by the ATLAS [48] and CMS [49] collaborations. We choose to simulate tag probabilities according to those given for the "DeepCSV Loose" category of [49]. Jets with $|\eta| < 2.5$ are flagged as b-tagged with probabilities that depend on their flavour at truth level as follows: truth b 85%, truth c 40%, truth light quark or gluon 1%. These tag probabilities are approximately independent of p_T and $|\eta|$. The relative uncertainty in the b-jet efficiency scale factors is around 1.5% and the uncertainties in the c-jet and light-jet mis-tag scale factors are around 4% and 10% respectively [50].

The value of $\not{E}_T$ is calculated from the vector sum at particle level of the p_T of all neutrinos in the event. Resolution in $\not{E}_T$ is taken into account by adding the difference between particle-level and detector level p_T of each lepton and jet in the event. We have checked that this procedure reproduces approximately the $\not{E}_T$ resolutions given in [52] and [54].

The effects of multiple proton–proton collisions or "pile-up" are not simulated in our study. In general, the lepton and jet identification algorithms employed by ATLAS and CMS are designed to have small pile-up dependence [55]. We take the performance values we have implemented to represent averages over the pile-up conditions experienced at the LHC.

References

1. 'Precision electroweak measurements on the Z resonance', ALEPH, DELPHI, L3, OPAL and SLD Collaborations, Phys. Rept. **427**, 257 (2006). https://doi.org/10.1016/j.physrep.2005.12.006
2. 'Electroweak Measurements in Electron-Positron Collisions at W-Boson-Pair Energies at LEP'. The ALEPH, DELPHI, OPAL and L3 Collaborations, Physics Reports **532**(4), 119–244 (2013). https://doi.org/10.1016/j.physrep.2013.07.004
3. M. Tanabashi et al., Review of Particle Physics'. The Particle Data Group. Phys. Rev. D **98**, 030001 (2018). https://doi.org/10.1103/PhysRevD.98.030001
4. V. Cirigliano, I. Rosell, 'Two-Loop Effective Theory Analysis of $\pi(K)\to e\overline{\nu}_e[\gamma]$ Branching Ratios'. Phys. Rev. Lett **99**, 231801 (2007). https://doi.org/10.1103/PhysRevLett.99.231801
5. Y. Amhis et al., 'Average of $R(D)$ and $R(D^*)$ for Spring 2019', Heavy Flavour Averaging Group (HFLAV), https://hflav-eos.web.cern.ch/hflav-eos/semi/spring19/html/RDsDsstar/RDRDs.html using the methods described. Eur. Phys. J. C **12**(77), 895 (2017). https://doi.org/10.1140/epjc/s10052-017-5058-4
6. J.P. Lees et al., Evidence for an excess of $\bar{B} \to D^{(*)}\tau^-\bar{\nu}_\tau$ decays', BaBar Collaboration. Phys. Rev. Lett. **109**, 101802 (2012). https://doi.org/10.1103/PhysRevLett.109.101802
7. J.P. Lees et al., Evidence for an excess of $\bar{B} \to D^{(*)}\tau^-\bar{\nu}_\tau$ decays and Implications for Charged Higgs Bosons', BaBar Collaboration. Phys. Rev. D **88**, 072012 (2013). https://doi.org/10.1103/PhysRevD.88.072012
8. M. Huschle et al., Measurement of the branching ratio of $\bar{B} \to D^{(*)}\tau^-\bar{\nu}_\tau$ relative to $\bar{B} \to D^{(*)}\ell^-\bar{\nu}_\ell$ decays with hadronic tagging at Belle', Belle Collaboration. Phys. Rev. D **92**, 072014 (2015). https://doi.org/10.1103/PhysRevD.92.072014
9. Y. Sato et al., 'Measurement of the branching ratio of $\bar{B}^0 \to D^{*+}\tau^-\bar{\nu}_\tau$ relative to $\bar{B}^0 \to D^{*+}\ell^-\bar{\nu}_\ell$ decays with a semileptonic tagging method', Belle Collaboration, Phys. Rev. D **94**, 072007 (2016). https://doi.org/10.1103/PhysRevD.94.072007
10. S. Hirose et al., 'Measurement of the τ lepton polarization and $R(D^*)$ in the decay $\bar{B} \to D^*\tau^-\bar{\nu}_\tau$', Belle Collaboration, Phys. Rev. Lett. **118**, 211801 (2017). https://doi.org/10.1103/PhysRevLett.118.211801
11. S. Hirose, 'Measurement of the τ lepton polarization and $R(D^*)$ in the decay $\bar{B} \to D^*\tau^-\bar{\nu}_\tau$ with one-prong hadronic τ decays at Belle', Belle Collaboration. Phys. Rev. D **97**, 012004 (2018). https://doi.org/10.1103/PhysRevD.97.012004
12. A. Abdesselam et al.,'Measurement of $R(D)$ and $R(D^*)$ with a semileptonic tagging method', Belle Collaboration, arXiv:1904.08794 [hep-ex]
13. R. Aaij et al., 'Measurement of the ratio of branching fractions $\mathcal{B}(\overline{B}^0 \to D^{*+}\tau^-\overline{\nu}_\tau)/\mathcal{B}(\overline{B}^0 \to D^{*+}\mu^-\overline{\nu}_\mu)$', LHCb Collaboration, Phys. Rev. Lett. **115**, 111803 (2015). https://doi.org/10.1103/PhysRevLett.115.111803 Erratum: Phys. Rev. Lett. **115**, 159901 (2015). https://doi.org/10.1103/PhysRevLett.115.159901
14. R. Aaij et al., Measurement of the ratio of the $B^0 \to D^{*-}\tau^+\nu_\tau$) and $B^0 \to D^{*-}\mu^+\nu_\mu$) branching fractions using three-prong τ-lepton decays', LHCb Collaboration, Phys. Rev. Lett. **120**, 171802 (2018). https://doi.org/10.1103/PhysRevLett.120.171802
15. R. Aaij et al., Test of lepton flavor universality by the measurement of the $B^0 \to D^{*-}\tau^+\nu_\tau$) branching fraction using three-prong τ decays', LHCb Collaboration, Phys. Rev. D **97**, 072013 (2018). https://doi.org/10.1103/PhysRevD.97.072013
16. N.B. LHCb measures the branching fractions for $\overline{B}^0 \to \tau^-\overline{\nu}_\tau D^+$ and $\overline{B}^0 \to \tau^-\overline{\nu}_\tau D^{*+}$ as ratios to the branching fractions for the decays $\overline{B}^0 \to \mu^-\overline{\nu}_\tau D^+$ and $\overline{B}^0 \to \mu^-\overline{\nu}_\tau D^{*+}$, rather than for an average of the e and μ decay modes, as is the case for BaBar and Belle
17. Y. Sakaki, M. Tanaka, A. Tayduganov, R. Watanabe, Testing leptoquark models in $\bar{B} \to D^{(*)}\tau\bar{\nu}$', Phys. Rev. D **88**, 094012 (2013). https://doi.org/10.1103/PhysRevD.88.094012
18. G. Aad et al., 'Measurement of the $W \to \tau\nu$ cross section in pp Collisions at $\sqrt{s} = 7TeV$ with the ATLAS experiment', ATLAS Collaboration, Phys. Lett. B **706**, 276 (2012). https://doi.org/10.1016/j.physletb.2011.11.057
19. G. Aad et al., 'Measurements of the top quark branching ratios into channels with leptons and quarks with the ATLAS detector',

ATLAS Collaboration, Phys. Rev. D **92**(7), 072005 (2015). https://doi.org/10.1103/PhysRevD.92.072005
20. V. Khachatryan et al., 'Measurement of the tt production cross section in pp collisions at $\sqrt{s} = 8\ TeV$ in dilepton final states containing one τ lepton', CMS Collaboration. Phys. Lett. B **739**, 23 (2014). https://doi.org/10.1016/j.physletb.2014.10.032
21. The pseudorapidity, η, is defined as $\eta = -\ln[\tan(\frac{\theta}{2})]$, where θ is the polar angle with respect to the beam direction, in the laboratory frame
22. G. Aad et al., Search for high-mass dilepton resonances using 139 fb^{-1} of pp collision data collected at $\sqrt{s}$ = 13 TeV with the ATLAS detector', ATLAS Collaboration, Phys. Lett. B **796**, 68 (2019). https://doi.org/10.1016/j.physletb.2019.07.016
23. G. Aad et al., Search for high-mass dilepton resonances using 139 fb^{-1} of pp collision data collected at $\sqrt{s}$ = 13 TeV with the ATLAS detector', ATLAS Collaboration, Phys. Lett. B **796**, 68 (2019). https://doi.org/10.1016/j.physletb.2019.07.016
24. G. Aad et al., 'Muon reconstruction performance of the ATLAS detector in proton-proton collision data at $\sqrt{s}$ = 13 TeV', ATLAS Collaboration, Eur. Phys. J. C **76**, 292 (2016). https://doi.org/10.1140/epjc/s10052-016-4120-y
25. A.M. Sirunyan et al., 'Performance of the CMS muon detector and muon reconstruction with proton-proton collisions at $\sqrt{s}$ = 13 TeV', CMS Collaboration, JINST **13**, P06015 (2018). https://doi.org/10.1088/1748-0221/13/06/P06015
26. G. Aad et al., 'Performance of the ATLAS trigger system in 2015', ATLAS Collaboration, Eur. Phys. J. C **77**, 317 (2017). https://doi.org/10.1140/epjc/s10052-017-4852-3
27. The efficiency of the single muon trigger has been measured in the barrel (endcap) region of CMS to be around 96% (90%)[24] and to be almost independent of p_T. In our simulation of the single muon trigger efficiency we choose to use the smaller values given in the text for ATLAS
28. 'Performance of electron and photon triggers in ATLAS during LHC Run 2', arXiv:1909.00761 [hep-ex]
29. M. Aaboud et al., 'Electron reconstruction and identification in the ATLAS experiment using the 2015 and 2016 LHC proton-proton collision data at $\sqrt{s} = 13\ TeV'$, ATLAS Collaboration, Eur. Phys. J. C **79**, 639 (2019). https://doi.org/10.1140/epjc/s10052-019-7140-6
30. A.M. Sirunyan et al., 'Performance of electron reconstruction and selection with the CMS detector in proton-proton collisions at $\sqrt{s} = 8\ TeV'$, CMS Collaboration, JINST **10**, P06005 (2015). https://doi.org/10.1088/1748-0221/10/06/P06005
31. For example, the region $1.37<|\eta|<1.52$ is usually excluded for precision measurements involving electrons or τ_{had}. We simulate this gap in this detector parameterisation
32. The efficiency for electron identification according for the "Tight likelihood" category is shown as functions of p_T and η in Figure 8 of[28]
33. We simulate approximately the efficiency for the single-electron trigger according to that given as a function of p_T in Figure 26 (a) of [25], except that the value of p_T on the abscissa is shifted up by 2 GeV to account for the fact that for most of the LHC run 2 the trigger threshold was set at $p_T = 26$ GeV [27]
34. M. Aaboud et al., 'Electron and photon energy calibration with the ATLAS detector using 2015–2016 LHC proton-proton collision data', ATLAS Collaboration, JINST **14**, P03017 (2019). https://doi.org/10.1088/1748-0221/14/03/P03017
35. The choice of 0.002 corresponds to a value in the middle of the range of values given in Table 2 of [33]
36. M. Aaboud et al.:'Electron efficiency measurements with the ATLAS detector using 2012 LHC proton-proton collision data', ATLAS Collaboration Eur. Phys. J. C **77**, 195 (2017). https://doi.org/10.1140/epjc/s10052-017-4756-2 An estimate of various sources of backgrounds to the sample of high p_T, isolated electron candidates in ATLAS is given in Table 3. The "Very tight likelihood" criterion in this paper has a very similar efficiency to "Tight likelihood" criterion in [28]. We, therefore, take the background probabilities given here for "Very tight likelihood" as being representative of those for the "Tight likelihood" in [28]
37. A.M. Sirunyan et al., 'Performance of reconstruction and identification of τ leptons decaying to hadrons and ν_τ in pp collisions at $\sqrt{s} = 13TeV'$, CMS Collaboration, JINST **13**, P10005 (2018). https://doi.org/10.1088/1748-0221/13/10/P10005
38. The τ_{had} identification efficiencies and jet fake probabilities corresponding to various working points of the MVA-based τ_{had} isolation algorithm are shown as a function of p_T in Figure 4 of [36]
39. The τ_{had} identification efficiencies and electron fake probabilities corresponding to various working points of the MVA-based electron discrimination algorithm are shown as a function of p_T in Figure 5 of [36]. The τ_{had} identification efficiencies and muon fake probabilities are given in section 5.4 of [36]
40. V. Khachatryan et al.: See Figure 8 (right) of 'Reconstruction and identification of τ lepton decays to hadrons and ν_τ at CMS', CMS Collaboration JINST **11**, P01019 (2016). https://doi.org/10.1088/1748-0221/11/01/P01019
41. The measurement in the CMS data of the probabilities for hadronic jets, electrons, and muons to be misidentified as τ_{had} candidates and comparison with MC simulations is described in section 10 of [36]
42. G. Aad et al., 'Measurement of the tau lepton reconstruction and identification performance in the ATLAS experiment using pp collisions at $\sqrt{s}$ = 13 TeV', ATLAS Collaboration, ATLAS-CONF-2017-029. http://cdsweb.cern.ch/record/2261772/files/ATLAS-CONF-2017-029.pdf
43. G. Aad et al., 'Reconstruction of hadronic decay products of tau leptons with the ATLAS experiment', ATLAS Collaboration. Eur. Phys. J. C **76**(5), 295 (2016). https://doi.org/10.1140/epjc/s10052-016-4110-0
44. In Figure 7 (left) of [36] the fraction of MJ background in the signal region of visible mass in the selected τ_{had} sample is seen to be around 20%, when using the "tight" operating point of the MVA-based τ_{had} identification algorithm and applying the "tight" isolation requirement to the muon. It can be seen from Figure 4 (left) of [36] that the signal efficiency for τ_{had} decreases by a factor of around 1.5 between the "tight" and "very-very-tight" operating points and from Figure 4 (right) of [36] that the background rejection improves by a factor of three. Therefore background to signal ratio improves by roughly a factor of two between the "tight" τ_{had} operating points. Similarly, in section 6.2 of [24] it is stated that the probability for a muon produced in a hadronic jet to satisfy tight isolation requirements is about 0.05 in the barrel, and goes up to about 0.15 in the endcap. This probability is around a factor of two larger than the probability of 0.03 that we have assumed for the probability for a muon produced in a hadronic jet. Taking these two factors of two into account we can, therefore, estimate the fraction of MJ background in the $Z \to \tau\tau \to \ell\tau_{\text{had}}$ sample selected using the "very-very-tight" operating point of the MVA-based τ_{had} identification algorithm and our chosen electron/muon isolation to be around $20/(2 \times 2) = 5\%$. The relative uncertainty on the MJ background quoted in section 9.1 of [36] is 5% and results from the limited size of the control samples in the $\int L\,dt = 36\text{fb}^{-1}$ of CMS data used in the measurement
45. M. Cacciari, G.P. Salam, G. Soyez, 'The anti-k_t jet clustering algorithm', JHEP **4**, 63 (2008). https://doi.org/10.1088/1126-6708/2008/04/063
46. M. Aaboud et al., 'Jet energy scale measurements and their systematic uncertainties in proton-proton collisions at $\sqrt{s}$ = 13 TeV with the ATLAS detector', ATLAS Collaboration, Phys. Rev. D **96**, 072002 (2017). https://doi.org/10.1103/PhysRevD.96.072002

47. V. Khachatryan et al., 'Jet energy scale and resolution in the CMS experiment in pp collisions at 8 TeV', CMS Collaboration, JINST **12**, P02014 (2017). https://doi.org/10.1088/1748-0221/12/02/P02014
48. G. Aad et al., 'Measurement of the b-jet identification efficiency at run-2 using tt events', ATLAS Collaboration, JHEP **2018**, 89 (2018). https://doi.org/10.1007/JHEP08(2018)089
49. A.M. Sirunyan, 'Identification of heavy-flavour jets with the CMS detector in pp collisions at 13 TeV', CMS Collaboration, JINST **13**, P05011 (2018). https://doi.org/10.1088/1748-0221/13/05/P05011
50. Tag probabilities for the "DeepCSV" tagging algorithms are shown as functions of p_T and η in Figure 17 of [48]. The data-simulation scale factors and their uncertainties are shown in Figure 53
51. M. Aaboud et al., 'Performance of missing transverse momentum reconstruction with the ATLAS detector using proton-proton collisions at $\sqrt{s}$ = 13 TeV', ATLAS Collaboration, Eur. Phys. J. **78**, 903 (2018). https://doi.org/10.1140/epjc/s10052-018-6288-9
52. Resolutions in $\not{E}_T$ as a function of $\not{E}_T$ for different physics processes are shown in Figure 9
53. A.M. Sirunyan et al., 'Performance of missing transverse momentum reconstruction in proton-proton collisions at $\sqrt{s}$ = 13 TeV using the CMS detector', CMS Collaboration, JINST **14**, P07004 (2019). https://doi.org/10.1088/1748-0221/14/07/P07004
54. Figure 10 shows the resolution of the $u_\parallel$ and $u_\perp$ components of the hadronic recoil. $u_\parallel$ and $u_\perp$ are defined in Figure 6
55. In particular, the efficiency of the DeepCSV Loose b-tagging algorithm of CMS has only a very moderate dependence on the number of pile-up interactions, as is shown in the top right-hand plot of Figure 17 of [48]. This means that the b-tagging requirements in the event selections will not introduce any significant difference in the pile-up distributions in the selected $t\bar{t} \to b\bar{b}W^+W^-$ and $Z/\gamma^* \to \tau\tau$ event samples
56. S. Alioli, P. Nason, C. Oleari, E. Re, 'A general framework for implementing NLO calculations in shower Monte Carlo programs: the POWHEG BOX', JHEP **1006**, 043 (2010). https://doi.org/10.1007/JHEP06(2010)043
57. T. Sjöstrand, S. Mrenna, 'A brief introduction to PYTHIA 8.1', Comput. Phys. Commun. **178**, 852 (2008). https://doi.org/10.1016/j.cpc.2008.01.036
58. E. Bothmann et al., 'Event Generation with Sherpa 2.2', SciPost Phys. **7**, 034 (2019). https://doi.org/10.21468/SciPostPhys.7.3.034
59. M. Aaboud et al., 'Measurement of differential W^+W^- production cross sections in proton-proton collisions at $\sqrt{s}$ = 13 TeV with the ATLAS detector', ATLAS Collaboration, Eur. Phys. J. C **79**, 884 (2019). https://doi.org/10.1140/epjc/s10052-019-7371-6
60. A.M. Sirunyan et al., 'Measurement of the tt production cross section, the top quark mass, and the strong coupling constant using dilepton events in pp collisions at $\sqrt{s}$ = 13 TeV', CMS Collaboration, Eur. Phys. J. **79**, 368 (2019). https://doi.org/10.1140/epjc/s10052-019-6863-8
61. Table 5 of [56] gives a number of predictions of the W^+W^- fiducial cross-section, with systematic uncertainties in the range 2–5%. Given that Z boson and EW diboson production are both dominated by $q\bar{q}$-initiated processes it is reasonable to assume that uncertainties due, e.g., to PDFs would at least partially cancel in the ratio. We assume an uncertainty of 3% on the ratio of the cross sections for Z boson and EW diboson production. In[57] the tt cross section is measured with a precision of around 3%. Since tt production is dominated by gluon-initiated processes we do not assume any cancellation of systematic uncertainties in evaluating the ratio to the Z boson cross section
62. G. Aad et al., 'Measurement of the transverse momentum and ϕ^*_η distributions of Drell-Yan lepton pairs in proton–proton collisions at $\sqrt{s} = 8\,TeV$ with the ATLAS detector', ATLAS Collaboration, Eur. Phys. J. C **76**(5), 291 (2016). https://doi.org/10.1140/epjc/s10052-016-4070-4
63. The assigned systematic uncertainties in our study correspond to the approximate size of the uncertainties on individual bins in $p_T(Z)$ in [59]. These are dominated by statistical uncertainties in the relevant region of $p_T(Z)$
64. G. Aad et al.,'Measurements of top-quark pair differential and double-differential cross-sections in the ℓ+jets channel with pp collisions at $\sqrt{s} = 13$ TeV using the ATLAS detector', ATLAS Collaboration, , arXiv:1908.07305 [hep-ex]
65. The systematic variations we simulate correspond approximately to the uncertainties on the measured distribution of $m(t\bar{t})$
66. A. Banfi, S. Redford, M. Vesterinen, P. Waller, T.R. Wyatt, 'Optimisation of variables for studying dilepton transverse momentum distributions at hadron colliders'. Eur. Phys. J. C **71**, 1600 (2011). https://doi.org/10.1140/epjc/s10052-011-1600-y
67. G. Aad et al., 'Measurement of the $Z/\gamma^* \to \tau\tau$ cross section with the ATLAS detector', ATLAS Collaboration, Phys. Rev. D **84**, 112006 (2011). https://doi.org/10.1103/PhysRevD.84.112006
68. M. Vesterinen, T.R. Wyatt, 'A Novel Technique for Studying the Z Boson Transverse Momentum Distribution at Hadron Colliders. Nucl. Instr. and Meth. A **602**, 432–437 (2009). https://doi.org/10.1016/j.nima.2009.01.203
69. To calculate the uncertainty from the alternative tt generator-level sample, equation 9 is modified to use the ratio of the efficiencies for selecting $tt \to bbe\mu$ and $tt \to bb\ell\tau_{\text{had}}$ events. The advantage of this modification is that the efficiencies have binomial uncertainties, which minimise the effects of statistical fluctuations in the alternative sample
70. M. Aaboud et al., 'Search for charged Higgs bosons decaying via $H^+ \to \tau^+\nu$ in the τ+ jets and τ+ lepton final states with 36 fb^{-1} of pp collision data recorded at $\sqrt{s} = 13\,TeV$ with the ATLAS experiment', ATLAS Collaboration, JHEP **1503**, 088 (2015). https://doi.org/10.1007/JHEP03(2015)088
71. V. Khachatryan et al., 'Search for a charged Higgs boson in pp collisions at $\sqrt{s} = 8\,TeV'$, CMS Collaboration, JHEP **1511**, 018 (2015). https://doi.org/10.1007/JHEP11(2015)018
72. M. Aaboud et al., 'Search for top-quark decays $t \to Hq$ with 36 fb^{-1} of pp collision data at $\sqrt{s}$ = 13 TeV with the ATLAS detector', ATLAS Collaboration, JHEP **1905**, 123 (2019). https://doi.org/10.1007/JHEP05(2019)123